Weierstraß-Institut
für Angewandte Analysis und Stochastik
Leibniz-Institut im Forschungsverbund Berlin e. V.

Preprint ISSN 2198-5855

Asymptotic study of the electric double layer at the interface of a polyelectrolyte gel and solvent bath

Matthew G. Hennessy[1], Giulia L. Celora[1], Andreas Münch[1], Sarah L. Waters[1],

Barbara Wagner[2]

submitted: August 19, 2020

[1] Mathematical Institute
Andrew Wiles Building, Woodstock Road
Oxford, OX2 6GG
UK
E-Mail: hennessy@maths.ox.ac.uk
celora@maths.ox.ac.uk
muench@maths.ox.ac.uk
waters@maths.ox.ac.uk

[2] Weierstrass Institute
Mohrenstr. 39
10117 Berlin
Germany
E-Mail: barbara.wagner@wias-berlin.de

No. 2751
Berlin 2020

2010 *Mathematics Subject Classification.* 74A30, 80A22, 34B15.

2010 *Physics and Astronomy Classification Scheme.* 83.80.Rs, 83.10.Tv.

Key words and phrases. Polyelectrolyte gel, phase separation, matched asymptotic expansions.

MH recognizes support from the Mathematical Institute through a Hooke fellowship, and GC acknowledges support through a Dphil scholarship from the SABS CDT, University of Oxford.

Edited by
Weierstraß-Institut für Angewandte Analysis und Stochastik (WIAS)
Leibniz-Institut im Forschungsverbund Berlin e. V.
Mohrenstraße 39
10117 Berlin
Germany

Fax: +49 30 20372-303
E-Mail: `preprint@wias-berlin.de`
World Wide Web: `http://www.wias-berlin.de/`

Asymptotic study of the electric double layer at the interface of a polyelectrolyte gel and solvent bath

Matthew G. Hennessy, Giulia L. Celora, Andreas Münch, Sarah L. Waters,

Barbara Wagner

Abstract

An asymptotic framework is developed to study electric double layers that form at the interface between a solvent bath and a polyelectrolyte gel that can undergo phase separation. The kinetic model for the gel accounts for the finite strain of polyelectrolyte chains, free energy of internal interfaces, and Stefan–Maxwell diffusion. By assuming that the thickness of the double layer is small compared to the typical size of the gel, matched asymptotic expansions are used to derive electroneutral models with consistent jump conditions across the gel-bath interface in two-dimensional plane-strain as well as fully three-dimensional settings. The asymptotic framework is then applied to cylindrical gels that undergo volume phase transitions. The analysis indicates that Maxwell stresses are responsible for generating large compressive hoop stresses in the double layer of the gel when it is in the collapsed state, potentially leading to localised mechanical instabilities that cannot occur when the gel is in the swollen state. When the energy cost of internal interfaces is sufficiently weak, a sharp transition between electrically neutral and charged regions of the gel can occur. This transition truncates the double layer and causes it to have finite thickness. Moreover, phase separation within the double layer can occur. Both of these features are suppressed if the energy cost of internal interfaces is sufficiently high. Thus, interfacial free energy plays a critical role in controlling the structure of the double layer in the gel.

1 Introduction

A polyelectrolyte gel in an ionic solvent bath represents a fundamental model system for innumerable biological problems, ranging from models for various subcellular processes, such as volume transitions of the nucleus or formation of organelles via liquid-liquid phase separation [5, 22], to models for cartilage or muscles tissue on the larger scale [21, 11]. Polyelectrolyte gels are thus fundamentally important to biomedical applications, where they are used as scaffolds for cell proliferation in regenerative medicine [17] and biocompatible systems for drug delivery [19]. Moreover, they are also becoming an important and novel material for soft actuators, fuel cells [15], or ionic devices such as polyelectrolyte gel diodes [29].

Mathematical modelling can provide unique insights into the structural and dynamic behaviour of polyelectrolyte gels and their dependence on the conditions of the surrounding solvent bath. Such models have been systematically derived using non-equilibrium thermodynamics [7, 10, 13, 2]. This approach enables thermodynamically consistent governing equations to be obtained from the combined free energy of the system, which generally accounts for the energy of mixing solvent, ions, and polyelectrolyte chains; the nonlinear elastic energy of polyelectrolyte chains, and the electrostatic energy.

In addition, apart from boundary conditions for a given geometry of the problem, interfacial conditions at the gel-bath interface need to be consistently formulated [8]. Typical problems focus on free or

DOI 10.20347/WIAS.PREPRINT.2751 Berlin 2020

constrained swelling, when a “dry” gel is immersed into a solvent bath. When the gel has attained its new swollen equilibrium state, electroneutrality of the gel and the surrounding bath is assumed, the so called Donnan equilibrium [9]. However, as either the dimensions of the gel and bath becomes very small or as the gel-bath interface is approached, this assumption is violated. An understanding of this transition is rooted in the problem of an electrolyte at a solid wall and how the mobile ions in the electrolyte arrange at the interface to achieve electroneutrality through the creation of a so-called electrical double layer. In general, the double layer consists of two parts. At the atomistic scale there is a monolayer of adsorbed and non-moving ions, the Stern or Helmholtz layer, to screen the charge at the wall. Adjacent to that is a diffusive layer, the so-called Debye layer, of mobile ions to compensate for the polarity and achieve neutrality in the bulk. The thickness of the Debye layer is typically about a few nanometers and depends on value of ion concentration or the fixed charges for polyelectrolytes. While the study of the Debye layer has been widespread, particularly in the context of applications in Li-ion batteries with electrolytes sandwiched between electrode walls [26, 18, 6], some of the more complete works analysing the asymptotic structure of the Debye layer as the Debye length decreases has been carried out by Richardson and King [24] and, in the context of electrophoresis, by Yariv *et al.* [30, 31] for the case of a flat, curved, and moving wall.

Double layers in polyelectrolyte gels are often not treated and electroneutrality is assumed, as for example in [32]. There are a few studies that explicitly consider the polyelectrolyte gel-bath double layer, such as in Hong *et al.* [13] and Wang and Hong [27] for freely swollen polyelectrolyte gels. Mori *et al.* [20] use matched asymptotics to derive jump conditions across the double layer but do not study the behaviour of solutions.

In this paper, we systematically develop an asymptotic framework to study electrical double layers in polyelectrolyte gels as the Debye length decreases. We compute solutions in two and three dimensions and derive electroneutral models with asymptotically consistent boundary conditions without restricting the modes of deformation that can occur. This work is based on a new model for polyelectrolyte gels, derived in [3], which accounts for the free energy of diffuse internal interfaces that form upon phase separation occurring within the gel. This can lead to different concentrations of solvent and ions in the phase-separated regions. As we have shown earlier for neutral hydrogels [12], it is necessary to include interfacial free energy in the model to capture the transient dynamics of these internal layers and how they that can be triggered by imposing a critical solvent flux into the gel. For polyelectrolyte gels, solvent flux into and out of the gel is more complex, since in addition it is intrinsically regulated via the concentrations of ions (salt) in the solvent bath, the amount of fixed charges on the polyelectrolyte chains, as well as (as for neutral hydrogels) the finite elasticity of the polyelectrolyte network. Internal phase-separated regions have been observed experimentally for some time and they are known to be quite sensitive to external conditions in the bath, as is the case for the well-known volume phase transition, or gel collapse [23]. As a consequence of our model, the asymptotic analysis reveals not only a small parameter characterising the small Debye length at the gel-bath interface, but, in addition, the thickness of the moving internal interfaces enters as a new small parameter into the asymptotic analysis.

We apply our formulation to the problem of a swelling cylindrical gel under axial compression. While our present asymptotic analysis considers only situations that deem the Debye length the smallest parameter, the additional terms that arise from the interfacial energy give rise to novel features such the formation of an interface between neutral and electrically charged regions of the gel. In addition, conditions for phase separation within a double layer are also discussed.

The paper is organised as follows. In Sec. 2 the governing equations for a polyelectrolyte gel that can undergo phase separation are presented along with those of the surrounding bath. In Sec. 3 we carry

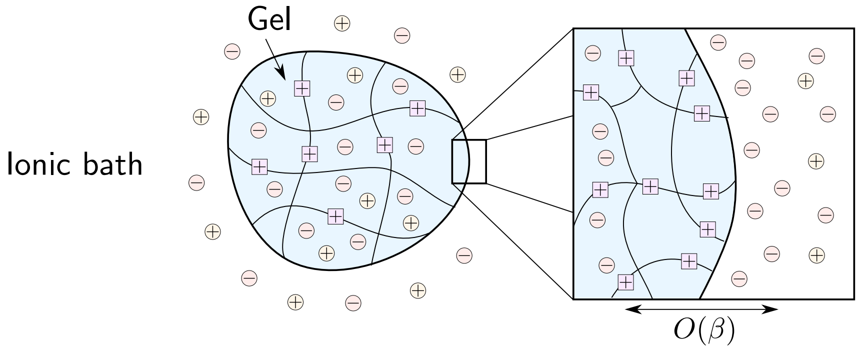

Figure 1: A swollen polyelectrolyte hydrogel surrounded by a bath. The bath consists of a dissolved binary salt. Here we assume the electric charges on the polymer chains of the gel are positive. Near the gel-bath interface, a thin electric double layer of thickness $O(\beta)$ forms where charge neutrality is violated. The definition of β is given in (1).

out an asymptotic analysis in three dimensions of the double layer that forms at the interface between the gel and bath. In Sec. 4, we present our analysis for a model that does not consider interfacial free energy. In Sec. 5, the asymptotics are specialised to a two-dimensional plane-strain setting. The asymptotic framework is then applied to swollen hydrogel cylinders in Sec. 6 and the paper concludes in Sec. 7.

2 Mathematical model

We consider a polyelectrolyte gel that is surrounded by a bath, as shown in Fig. 1. The bath consists of a solvent and a dissolved binary salt such as NaCl or $\mathrm{CaCl_2}$. The gel is composed of a crosslinked network of deformable polymer chains that carry electric charges of the same sign. Changes in the salt concentration in the bath will drive solution (solvent and ions) into or out of the gel through osmosis and potentially trigger the formation of diffuse internal interfaces within the gel through phase transitions and/or phase separation [4].

A phase-field model for a polyelectrolyte gel undergoing phase separation has been systematically derived by Celora *et al.* [3] using non-equilibrium thermodynamics. This model will form the basis of the present study. For brevity, we only present the non-dimensional form of the governing equations in the main text; however, the dimensional model is provided in Appendix A. In the equations below, the subscript m is used to represent quantities associated with the solvent (s), cation ($+$), or the anion ($-$). The subscript n refers to the polymer network. The set $\mathbb{M} = \{s, +, -\}$ contains all of the mobile species that move relative to the polymer chains. We let $\mathbb{I} = \{+, -\}$ denote the ionic species.

In non-dimensionalising the model, spatial variables are scaled with a characteristic length scale L, which, for example, might represent the size of the gel in its dry or as-prepared states. Similarly, the displacement of solid elements, $\boldsymbol{a}$, is scaled with $\boldsymbol{a} \sim L$. We choose a time scale associated with solvent diffusion in the gel, $t \sim L^2/D_s^0$ where D_s^0 is a reference value of the diffusivity. This time scale imparts a velocity scale for each species: $\boldsymbol{v}_k \sim D_s^0/L$. The chemical potentials of the mobile species are written as $\mu_m = \mu_m^0 + k_B T \mu_m'$, where μ_m^0 is a reference chemical potential, k_B is Boltzmann's constant, and T is the absolute temperature. The diffusives fluxes in the gel and the bath scale like $\boldsymbol{j}_m \sim D_s^0 \nu^{-1}/L$ and $\boldsymbol{q}_m \sim D_s^0 \nu^{-1}/L$, respectively, where ν is a typical molecular volume (assumed to the be same for each mobile species). The electric potential in the bath and the gel is scaled with the thermal voltage, $\Phi \sim k_B T/e$, where e is the elementary charge. Pressure gradients in the gel are assumed to balance the elastic stress, $p \sim G$, where G is the shear modulus of the polymer network. In the bath, pressure gradients are balanced with the Maxwell stress, leading to

$p \sim \epsilon^{\text{bath}}(k_B T/e)^2/L^2$, with ϵ^{bath} denoting the electrical permitivity of the bath, which is assumed to be constant.

This scaling introduces four key dimensionless parameters given by

$$\mathcal{G} = \frac{\nu G}{k_B T}, \quad \omega = \frac{1}{L}\left(\frac{\gamma}{\nu k_B T}\right)^{1/2}, \quad \beta = \frac{1}{L}\left(\frac{\nu \epsilon^{\text{gel}} k_B T}{e^2}\right)^{1/2}, \quad \mathcal{N} = \frac{\eta D_s}{\epsilon^{\text{bath}}(k_B T/e)^2}, \tag{1}$$

where η is the kinematic viscosity of the solution (assumed constant) and γ is related to the free energy cost of internal interfaces. The parameter $\mathcal{G}$ characterises the energetic cost of elastically deforming the gel relative to the energy that is released upon insertion of a solvent molecule. The parameters ω and β describe the thickness of diffuse internal interfaces and electrical double layers relative to L, respectively. Finally, $\mathcal{N}$ represents the ratio of the viscous stress to the Maxwell stress in the bath. The magnitudes of these numbers will be estimated in Sec. 2.4.

2.1 Governing equations for the gel

The governing equations for the gel are formulated in terms of Eulerian coordinates $\boldsymbol{x} = x_i \boldsymbol{e}_i$ associated with the current state of the system, where $\boldsymbol{e}_i$ are Cartesian basis vectors. This choice of coordinate system enables the equations to be written in a physically intuitive way and allows for a straightforward interpretation of geometric quantities associated with the gel-bath interface (e.g. curvature). A detailed account of Eulerian-based hydrogel modelling is provided by Bertrand *et al.* [1]. In Eulerian coordinates, the deformation gradient tensor F, which describes the distortion of material elements relative to the dry state of the gel, is more readily expressed through its inverse,

$$\mathsf{F}^{-1} = \nabla \boldsymbol{X}, \tag{2}$$

where $\boldsymbol{X}(\boldsymbol{x}, t) = X_I \boldsymbol{E}_I$ are Lagrangian coordinates associated with the reference (dry) state of the gel, $\boldsymbol{E}_I$ are Cartesian basis vectors in the reference state, and $\nabla = \boldsymbol{e}_i\, \partial/\partial x_i$. The adopted conventions for computing derivatives of vectors and tensors are given in Appendix B. The quantity $\boldsymbol{X}(\boldsymbol{x}, t)$ provides the Lagrangian coordinates of the material element that is located at the point $\boldsymbol{x}$ in the current state at time t. We assume that the basis vectors $\boldsymbol{e}_i$ and $\boldsymbol{E}_i$ have the same origin and direction. The Eulerian displacement is given by $\boldsymbol{a}(\boldsymbol{x}, t) = \boldsymbol{x} - \boldsymbol{X}(\boldsymbol{x}, t)$. Thus, the deformation gradient tensor F, is linked to the solid displacement $\boldsymbol{a}$ according to

$$\mathsf{F}^{-1} = \mathsf{I} - \nabla \boldsymbol{a}, \tag{3}$$

The determinant $J = \det \mathsf{F}$ characterises volumetric changes in material elements. Both the polymer chains and the interstitial fluid are assumed to be incompressible. As a result, any volumetric change in a solid element must be due to a variation in the amount of fluid contained within that element. This leads to the so-called molecular incompressibility condition

$$J = \left(1 - \sum_{m \in \mathbb{M}} \phi_m\right)^{-1} = \phi_n^{-1}, \tag{4}$$

where ϕ_k represent the volume fraction of species k. The volume of fixed charges on the polymer chains is accounted for in the network fraction ϕ_n. Since J describes the volume of swollen material elements relative to their dry volume, we also refer to it as the swelling ratio. The velocity of the solid elements $\boldsymbol{v}_n$ is related to the displacement via

$$\boldsymbol{v}_n = \mathsf{F}\, \frac{\partial \boldsymbol{a}}{\partial t}. \tag{5}$$

Conservation of polymer, solvent, and ions leads to

$$\frac{\partial \phi_n}{\partial t} + \nabla \cdot (\phi_n \boldsymbol{v}_n) = 0, \tag{6a}$$

$$\frac{\partial \phi_m}{\partial t} + \nabla \cdot (\phi_m \boldsymbol{v}_n + \boldsymbol{j}_m) = 0, \tag{6b}$$

where $\boldsymbol{j}_m = \phi_m(\boldsymbol{v}_m - \boldsymbol{v}_n)$ is the diffusive flux and $m \in \mathbb{M}$. The mixture velocity in the gel is defined as, and satisfies,

$$\boldsymbol{v} \equiv \phi_n \boldsymbol{v}_n + \sum_{m\in\mathbb{M}} \phi_m \boldsymbol{v}_m = \boldsymbol{v}_n + \sum_{m\in\mathbb{M}} \boldsymbol{j}_m. \tag{7}$$

Diffusive transport of solvent and ions is modelled using a Stefan–Maxwell approach. This enables multi-component diffusion to be captured by linking each diffusive flux to every chemical potential gradient. The fluxes are thus given by

$$\boldsymbol{j}_s = -\mathcal{D}_s(J) \sum_{m\in\mathbb{M}} \phi_m \nabla \mu_m, \tag{8a}$$

$$\boldsymbol{j}_\pm = -\mathcal{D}_\pm \phi_\pm \nabla \mu_\pm + \frac{\phi_\pm}{\phi_s} \boldsymbol{j}_s, \tag{8b}$$

where $\mathcal{D}_s(J) = D_s(J)/D_s^0$ and $\mathcal{D}_\pm = D_\pm/D_s^0$. The dimensional parameters D_s and $D_\pm$ denote the solvent diffusivity relative to the polymer network and the ionic diffusivity relative to a pure solvent bath, respectively. The dependence of $\mathcal{D}_s$ on J reflects the change in diffusivity (or permeability) that occurs as the polymer network is deformed [1]. The chemical potentials can be written as

$$\mu_s = \Pi_s + \mathcal{G}p - \omega^2 \nabla^2 \phi_s, \tag{9a}$$

$$\mu_\pm = \Pi_\pm + \mathcal{G}p + z_\pm \Phi, \tag{9b}$$

where $z_\pm$ is the valence of the ions and Π_m are osmotic pressures defined as

$$\Pi_s = \log \phi_s + \chi\, J^{-1}(1 - \phi_s) + J^{-1}, \tag{10a}$$

$$\Pi_\pm = \log \phi_\pm + J^{-1}(1 - \chi \phi_s). \tag{10b}$$

Here, χ is the Flory interaction parameter, which describes (unfavourable) enthalpic interactions between the solvent molecules and the polymer chains. The electric potential satisfies

$$-\beta^2 \nabla^2 \Phi = z_+ \phi_+ + z_- \phi_- + z_f \phi_f, \tag{11}$$

where ϕ_f represents the volume fraction of fixed charges on the polymer network and z_f denotes the valence of these charges. The nominal volume fraction of fixed charges is $C_f = \phi_f J$. In writing (11), we have assumed that the electrical permittivity of the gel is constant.

The conservation of linear momentum in the gel leads to

$$\nabla \cdot \mathbf{T} = 0, \tag{12}$$

where $\mathbf{T}$ is the Cauchy stress tensor, which can be decomposed according to

$$\mathbf{T} = \mathbf{T}_e + \mathbf{T}_K + \mathbf{T}_M - p\mathbf{I}. \tag{13a}$$

The first contribution, $\mathbf{T}_e$, represents the elastic stress tensor and is calculated by assuming the polymer chains behave as a neo-Hookean material. This leads to

$$\mathbf{T}_e = J^{-1}(\mathbf{B} - \mathbf{I}), \tag{13b}$$

where $\mathbf{B} = \mathbf{F}\mathbf{F}^T$ is the left Cauchy-Green deformation tensor. The second and third contributions, $\mathbf{T}_K$ and $\mathbf{T}_M$, correspond to the Korteweg and Maxwell stress tensors, respectively, which capture the force generated within the bulk of the hydrogel due to internal interfaces and electric fields. These tensors can be written as

$$\mathbf{T}_K = \mathcal{G}^{-1}\omega^2\left[\left(\frac{1}{2}|\nabla\phi_s|^2 + \phi_s\nabla^2\phi_s\right)\mathbf{I} - \nabla\phi_s \otimes \nabla\phi_s\right], \tag{13c}$$

$$\mathbf{T}_M = \mathcal{G}^{-1}\beta^2\left(\nabla\Phi \otimes \nabla\Phi - \frac{1}{2}|\nabla\Phi|^2\mathbf{I}\right). \tag{13d}$$

The final contribution to the Cauchy stress tensor represents an isotropic stress induced by the fluid pressure.

2.2 Governing equations for the bath

Conservation of solvent and ions in the bath is given by

$$\frac{\partial\phi_m}{\partial t} + \nabla\cdot(\phi_m\boldsymbol{v} + \boldsymbol{q}_m) = 0, \tag{14}$$

where $m \in \mathbb{M}$, $\boldsymbol{v}$ is the mixture velocity

$$\boldsymbol{v} = \sum_{m\in\mathbb{M}} \phi_m\boldsymbol{v}_m, \tag{15}$$

and $\boldsymbol{q}_m = \phi_m(\boldsymbol{v}_m - \boldsymbol{v})$ are the diffusive fluxes. Unlike the gel, the diffusive fluxes in the bath are defined relative to the mixture velocity. The bath is assumed to be free of voids and incompressible, which leads to the following conditions:

$$\sum_{m\in\mathbb{M}} \phi_m = 1, \qquad \nabla\cdot\boldsymbol{v} = 0. \tag{16}$$

The diffusive fluxes in the bath are also obtained using a Stefan–Maxwell approach and given by

$$\boldsymbol{q}_\pm = -\mathcal{D}_\pm\phi_\pm\left(\nabla\mu_\pm - \sum_{m\in\mathbb{M}}\phi_m\nabla\mu_m\right) + \frac{\phi_\pm}{\phi_s}\boldsymbol{q}_s, \tag{17a}$$

$$\boldsymbol{q}_s = -\boldsymbol{q}_+ - \boldsymbol{q}_-. \tag{17b}$$

The chemical potentials of the solvent and ions are

$$\mu_s = \log\phi_s + \epsilon_r\beta^2 p, \tag{18a}$$

$$\mu_\pm = \log\phi_\pm + \epsilon_r\beta^2 p + z_\pm\Phi, \tag{18b}$$

where $\epsilon_r = \epsilon^{\text{bath}}/\epsilon^{\text{gel}}$. The electric potential satisfies

$$-\epsilon_r\beta^2\nabla^2\Phi = z_+\phi_+ + z_-\phi_-. \tag{19}$$

Conservation of linear momentum in the bath implies that

$$\nabla \cdot \mathbf{T} = 0, \tag{20}$$

where the Cauchy stress tensor is

$$\mathbf{T} = \mathbf{T}_v + \mathbf{T}_M - p\mathbf{I}. \tag{21a}$$

The first component captures the viscous stresses in the bath, which is assumed to be a Newtonian fluid; thus,

$$\mathbf{T}_v = \mathcal{N}(\nabla \boldsymbol{v} + \nabla \boldsymbol{v}^T). \tag{21b}$$

The Maxwell stress tensor for the bath reads

$$\mathbf{T}_M = \nabla\Phi \otimes \nabla\Phi - \frac{1}{2}|\nabla\Phi|^2\mathbf{I}. \tag{21c}$$

By combining (20)–(21), we can write the stress balance in non-conservative form,

$$\nabla \cdot \mathbf{T}_v + \nabla^2\Phi\nabla\Phi = \nabla p, \tag{22}$$

which will be advantageous for the asymptotic analysis of the double layer.

2.3 Boundary conditions at the gel-bath interface

The gel-bath interface is defined by the surface $\boldsymbol{x} = \boldsymbol{r}(s_1, s_2, t)$, where s_1 and s_2 are parameters. The tangent vectors to the interface are defined as $\boldsymbol{t}_i = \partial\boldsymbol{r}/\partial s_i$. The normal vector to this surface is denoted by $\boldsymbol{n} = (\boldsymbol{t}_1 \times \boldsymbol{t}_2)/|\boldsymbol{t}_1 \times \boldsymbol{t}_2|$ and assumed to point from the gel into the bath. The normal velocity of the interface is written as V_n. We use the notation $\boldsymbol{x} \to \boldsymbol{r}^{\pm}$ to denote approaching the interface from the interior of the bath $(+)$ and gel $(-)$.

The kinematic boundary condition is imposed on the polymer network

$$[\boldsymbol{v}_n \cdot \boldsymbol{n} - V_n]_{\boldsymbol{x}=\boldsymbol{r}^-} = 0. \tag{23}$$

Conservation of solvent and ions across the moving boundary of the gel implies that

$$[\boldsymbol{j}_m \cdot \boldsymbol{n}]_{\boldsymbol{x}=\boldsymbol{r}^-} = A_m = [\boldsymbol{q}_m \cdot \boldsymbol{n} + \phi_m(\boldsymbol{v}_m \cdot \boldsymbol{n} - V_n)]_{\boldsymbol{x}=\boldsymbol{r}^+}\,, \tag{24}$$

where the A_m are introduced to facilitate the asymptotic matching in Sec. 3. By summing (24) over $m \in \mathbb{M}$ and using (7) and (23), we find that the normal component of the mixture velocity is continuous at the interface,

$$[\boldsymbol{v} \cdot \boldsymbol{n}]_{\boldsymbol{x}=\boldsymbol{r}^-} = [\boldsymbol{v} \cdot \boldsymbol{n}]_{\boldsymbol{x}=\boldsymbol{r}^+}\,, \tag{25}$$

which is a reflection of the conservation of total mass.

Continuity of the chemical potential across the interface leads to

$$\mu_m|_{\boldsymbol{x}=\boldsymbol{r}^-} = M_m = \mu_m|_{\boldsymbol{x}=\boldsymbol{r}^+}\,. \tag{26}$$

Due to the non-local term in the solvent chemical potential (9a), an additional boundary condition on the solvent fraction in the gel is required. We impose the variational condition

$$[\nabla\phi_s \cdot \boldsymbol{n}]_{\boldsymbol{x}=\boldsymbol{r}^-} = 0. \tag{27}$$

From a physical point of view, this condition implies that the solvent does not preferentially wet or dewet the interface, both of which would lead to a localised gradient in the solvent composition.

After non-dimensionalisation, momentum conservation at the interface leads to

$$[\mathcal{G}\mathsf{T} \cdot \boldsymbol{n}]_{\boldsymbol{x}=\boldsymbol{r}^-} = \left[\epsilon_r\beta^2\mathsf{T} \cdot \boldsymbol{n}\right]_{\boldsymbol{x}=\boldsymbol{r}^+}. \tag{28}$$

However, the asymptotic analysis will reveal that the stresses in the bath are $O(\beta^{-1})$ in size. Typically, $\beta \ll \mathcal{G}$, meaning that (28) can be reduced to a stress-free condition for the gel:

$$[\mathsf{T} \cdot \boldsymbol{n}]_{\boldsymbol{x}=\boldsymbol{r}^-} = 0. \tag{29}$$

The final boundary condition that must be imposed on the mechanical problem is a form of slip condition. Due to the various velocities in the model (e.g. solvent, mixture), there is a wide range of conditions that could be imposed. For instance, Mori *et al.* [20] considered a Navier slip condition on the solvent velocity in their kinetic model of a polyelectrolyte gel. The choice of boundary condition is relatively immaterial for this paper and thus we simply impose continuity of the tangential components of the mixture velocity:

$$[\boldsymbol{v} \cdot \boldsymbol{t}_i]_{\boldsymbol{x}=\boldsymbol{r}^-} = U_i = [\boldsymbol{v} \cdot \boldsymbol{t}_i]_{\boldsymbol{x}=\boldsymbol{r}^+}. \tag{30}$$

We assume there are no surface charges on the interface and therefore impose continuity of the electric potential and electric displacement:

$$\Phi|_{\boldsymbol{x}=\boldsymbol{r}^-} = \Phi|_{\boldsymbol{x}=\boldsymbol{r}^+}, \tag{31a}$$

$$[\nabla\Phi \cdot \boldsymbol{n}]_{\boldsymbol{x}=\boldsymbol{r}^-} = [\epsilon_r\nabla\Phi \cdot \boldsymbol{n}]_{\boldsymbol{x}=\boldsymbol{r}^+}. \tag{31b}$$

2.4 Parameter estimation

We assume that the molecular volume of solvent and ions is $\nu \sim 10^{-28}$ m^3 [32], the system is held at a temperature of $T = 300$ K, and the gels have a length scale of $L \sim 1$ cm. Horkay *et al.* [14] measured the shear moduli of polyelectrolyte gels to be around $G \sim 10$ kPa, which leads to $\mathcal{G} \sim 10^{-4}$. Yu *et al.* [32] report values of $\mathcal{G} \sim 10^{-3}$.

Assuming the electrical permittivity of the gel is approximately the same as water, $\epsilon^{\text{gel}} \simeq 80\,\epsilon_0$, where ϵ_0 is the permittivity of free space, then the non-dimensional width of the electrical double layers is $\beta \sim 10^{-8}$, corresponding to a dimensional length of 0.1 nm. However, we will show in Sec. 6 that these values underestimate the width of double layers computed from the model.

The dimensionless parameter ω is difficult to directly estimate due to uncertainty in the value of γ, the latter of which characterises the energy cost of diffuse internal interfaces. However, the quantity ω/β represents the relative width of diffuse interfaces to electrical double layers in the gel. Given the smallness of β, it is reasonable to expect that $\omega = O(\beta)$ or $\omega \gg \beta$. In this paper, we mainly focus on the case of $\omega \gg \beta$. For comparison purposes, we also consider the case where interfacial free energy is neglected, $\omega = 0$, as this is more common in the literature.

Drozdov *et al.* [10] report solvent diffusion coefficients ranging from $D_s^0 \sim 10^{-11}$ m^2·s^{-1} to $D_s \sim 10^{-9}$ m^2·s^{-1}. In a dilute solution, the ionic diffusivities are on the order of $D_\pm \sim 10^{-9}$ m^2·s^{-1} [25]. Thus, we expect $\mathcal{D}_\pm$ to range from 1 to 100. Assuming the solvent is water, which has a viscosity $\eta \sim 10^{-3}$ Pa·s, then we find that $\mathcal{N}$ ranges from 10^{-2} to 1. The (nominal) volume fraction of fixed charges is reported to range from $C_f \sim 10^{-3}$ to $C_f \sim 10^{-1}$ [13, 32]. The Flory interaction parameter χ is treated as a constant for simplicity; however, its value has been reported to range from 0.1 to 2.3 [32].

3 Asymptotic analysis of the model

The smallness of β implies, from (11) and (19), that material elements will be electrically neutral except in thin electric double layers of width $O(\beta)$ that form near interfaces. The onset of phase separation within the gel will create internal interfaces and hence leads to the possibility of internal double-layer formation. However, by assuming that $\omega \gg \beta$, we can rule out this possibility, as the interfaces that form by phase separation will be too wide to generate electric fields that are strong enough to violate electroneutrality. Thus, the only double layer in the system will occur at the gel-bath interface.

With this in mind, we now consider the asymptotic limit as $\beta \to 0$ with $\omega = O(1)$. This singular limit divides the domain of the problem into two main regions. In the outer region, away from the gel-bath interface, charge neutrality will hold in the gel and bath. The inner region is localised to the gel-bath interface and captures the electric double layer where charge neutrality is violated.

The asymptotic analysis is split into three parts. In Sec. 3.1, we reduce the model in the outer region away from the gel-bath interface and in doing so formulate the bulk equations for an electroneutral model. In Sec. 3.2, we formulate the problem in the inner region to resolve the features of the double layer. Finally, in Sec. 3.3, we asymptotically match the solutions in the inner and outer regions in order to derive consistent boundary conditions for the electroneutral model.

3.1 The outer problem

3.1.1 Electroneutral equations for the bath

Taking $\beta \to 0$ in (19) leads to the electroneutrality condition

$$z_+\phi_+ + z_-\phi_- = 0. \tag{32}$$

When (32) is combined with the no-void condition (16), the volume fractions of solvent ϕ_s and anions ϕ_- can be eliminated from the problem. By manipulating the ion balances in (14), we can arrive at

$$\nabla \cdot \big(z_+\boldsymbol{q}_+ + z_-\boldsymbol{q}_-\big) = 0, \tag{33}$$

which we interpret as an elliptic equation for the electric potential Φ in the bath. The volume fraction of cation evolves according to

$$\frac{\partial \phi_+}{\partial t} + \boldsymbol{v} \cdot \nabla\phi_+ + \nabla \cdot \boldsymbol{q}_+ = 0. \tag{34}$$

The fluxes in the bath are given by (17) and the chemical potentials reduce to

$$\mu_s = \log\phi_s, \tag{35a}$$

$$\mu_\pm = \log\phi_\pm + z_\pm\Phi, \tag{35b}$$

which show that the contribution from the pressure can be neglected. Finally, the mixture velocity $\boldsymbol{v}$ satisfies

$$\mathcal{N}\nabla^2\boldsymbol{v} + \nabla^2\Phi\nabla\Phi = \nabla p, \tag{36a}$$

$$\nabla\cdot\boldsymbol{v} = 0, \tag{36b}$$

where $\mathcal{N}$ has been assumed to be independent of composition.

3.1.2 Electroneutral equations for the gel

Taking $\beta \to 0$ in (11) leads to the electroneutrality condition in the gel,

$$z_+\phi_+ + z_-\phi_- = -z_f\phi_f. \tag{37}$$

Using $\phi_f = C_f/J$ along with (4) in (37), the anion fraction ϕ_- can be eliminated from the outer problem. By multiplying the conservation equation for each ion by their respective valence number z_i and adding, we find that

$$\nabla\cdot(z_+\boldsymbol{j}_+ + z_-\boldsymbol{j}_-) = z_f\left(\frac{\partial\phi_f}{\partial t} + \nabla\cdot(\phi_f\boldsymbol{v}_n)\right) = 0, \tag{38}$$

which determines the electric potential in the gel. The second equality is obtained by writing $\phi_f = C_f/J$, assuming that C_f is uniform, and then using the identity

$$\frac{\partial J}{\partial t} + \boldsymbol{v}_n\cdot\nabla J = J\nabla\cdot\boldsymbol{v}_n. \tag{39}$$

The solvent and cation fractions satisfy the equations

$$\frac{\partial\phi_s}{\partial t} + \nabla\cdot(\phi_s\boldsymbol{v}_n + \boldsymbol{j}_s) = 0, \tag{40a}$$

$$\frac{\partial\phi_+}{\partial t} + \nabla\cdot\left(\phi_+\boldsymbol{v}_n + \boldsymbol{j}_+\right) = 0, \tag{40b}$$

where the fluxes and chemical potentials are given by (8)–(10). The network velocity $\boldsymbol{v}_n$ is obtained by solving the mechanical problem, which consists of the kinematic relations in (3) and (5) and the stress balance

$$\nabla\cdot\mathbf{T}_e + \omega^2\mathcal{G}^{-1}\phi_s\nabla\nabla^2\phi_s = \nabla p, \tag{41}$$

where the elastic stress tensor is given by (13b). The form of (41) shows that the Maxwell stresses in the gel are negligible away from the gel-bath interface.

3.2 The inner problem

To solve the inner problem, we make the change of variable

$$\boldsymbol{x} = \boldsymbol{r}(s_1, s_2, t') + \beta\xi\boldsymbol{n}(s_1, s_2, t'), \quad t = t', \tag{42}$$

where ξ is a coordinate in the normal direction, with $\xi > 0$ corresponding to the regions in the bath whereas $\xi < 0$ corresponding to regions in the gel. Under this change of variable, the spatial and time derivatives become (see Appendix C for details)

$$\nabla = \beta^{-1}\boldsymbol{n}\frac{\partial}{\partial\xi} + \nabla_s + O(\beta), \tag{43a}$$

$$\nabla^2 = \beta^{-2}\frac{\partial^2}{\partial\xi^2} + 2\beta^{-1}\kappa\frac{\partial}{\partial\xi} + \nabla_s^2 - \xi(\kappa_i\kappa_i)\frac{\partial}{\partial\xi} + O(\beta), \tag{43b}$$

$$\frac{\partial}{\partial t} = -\beta^{-1}V_n\frac{\partial}{\partial\xi} + O(1), \tag{43c}$$

where ∇_s and ∇_s^2 are the surface gradient and surface Laplacian, defined in (158) and (164); κ_1 and κ_2 are the principal curvatures of the interface; and $\kappa = (\kappa_1 + \kappa_2)/2$ is the mean curvature. In deriving (43), we have assumed that the non-dimensional curvatures satisfy $\kappa_i = O(1)$ as $\beta \to 0$, i.e. the dimensional curvature is $O(L^{-1})$ where L is the typical length scale of the gel.

Tildes are used to denote dependent variables in the inner region, which are generally expanded as $\tilde{f} = \tilde{f}^{(0)} + \beta\tilde{f}^{(1)} + O(\beta^2)$, where f is an arbitrary quantity (scalar, vector, tensor). However, additional rescaling is required in some cases; this will be made explicit in the proceeding discussion. Near the interface, the outer solutions for the bath and gel expanded as

$$\lim_{\xi\to 0^+} f(\boldsymbol{r} + \beta\xi\boldsymbol{n}, t) = f^{\text{bath}}(\boldsymbol{r}, t) + O(\beta), \tag{44a}$$

$$\lim_{\xi\to 0^-} f(\boldsymbol{r} + \beta\xi\boldsymbol{n}, t) = f^{\text{gel}}(\boldsymbol{r}, t) + O(\beta), \tag{44b}$$

which will be used for asymptotic matching.

3.2.1 Inner problem for the bath

Mass conservation The $O(\beta^{-1})$ contributions to (14) in inner coordinates must satisfy

$$-V_n\frac{\partial\tilde{\phi}_m^{(0)}}{\partial\xi} + \frac{\partial}{\partial\xi}\left(\tilde{\phi}_m^{(0)}\tilde{\boldsymbol{v}}^{(0)}\cdot\boldsymbol{n} + \tilde{\boldsymbol{q}}_m^{(0)}\cdot\boldsymbol{n}\right) = 0, \tag{45}$$

where we have used the fact that $\boldsymbol{n}$ is independent of ξ. Integrating these equations gives

$$\tilde{\boldsymbol{q}}_m^{(0)}\cdot\boldsymbol{n} + \tilde{\phi}_m^{(0)}\left(\tilde{\boldsymbol{v}}^{(0)}\cdot\boldsymbol{n} - V_n\right) = A_m(s_1, s_2, t) \tag{46}$$

where the integration constant A_m is determined by matching to the outer solution:

$$A_m(s_1, s_2, t) = \boldsymbol{q}_m^{\text{bath}}\cdot\boldsymbol{n} + \phi_s^{\text{bath}}(\boldsymbol{v}_m^{\text{bath}}\cdot\boldsymbol{n} - V_n). \tag{47}$$

The leading-order part of the incompressibility condition for the bath (16) is given by

$$\frac{\partial}{\partial\xi}\left(\tilde{\boldsymbol{v}}^{(0)}\cdot\boldsymbol{n}\right) = 0. \tag{48}$$

Integrating and matching to the outer solution as $\xi \to \infty$ gives

$$\tilde{\boldsymbol{v}}^{(0)}\cdot\boldsymbol{n} = \boldsymbol{v}^{\text{bath}}\cdot\boldsymbol{n}. \tag{49}$$

Momentum conservation We rescale the pressure, Maxwell stress tensor, and viscous stress tensor according to $p = \beta^{-2}\tilde{p}$, $\mathbf{T}_M = \beta^{-2}\tilde{\mathbf{T}}_M$, and $\mathbf{T}_v = \beta^{-1}\tilde{\mathbf{T}}_v$. Consequently, the Cauchy stress tensor must be scaled as $\mathbf{T} = \beta^{-2}\tilde{\mathbf{T}}$. The local form of the stress balance (22) is given by

$$\begin{aligned}\beta\frac{\partial}{\partial\xi}\left(\tilde{\mathbf{T}}_v^{(0)}\cdot\boldsymbol{n}\right) + \frac{\partial\tilde{\Phi}^{(0)}}{\partial\xi}\frac{\partial^2\tilde{\Phi}^{(0)}}{\partial\xi^2}\boldsymbol{n} - 2\beta\kappa\left(\frac{\partial\tilde{\Phi}^{(0)}}{\partial\xi}\right)^2\boldsymbol{n}& \\ + \beta\frac{\partial\tilde{\Phi}^{(0)}}{\partial\xi}\frac{\partial^2\tilde{\Phi}^{(1)}}{\partial\xi^2}\boldsymbol{n} = \frac{\partial\tilde{p}^{(0)}}{\partial\xi}\boldsymbol{n} + \beta\frac{\partial\tilde{p}^{(1)}}{\partial\xi}\boldsymbol{n} + \nabla_s\tilde{p}^{(0)} + O(\beta^2).& \qquad (50)\end{aligned}$$

The $O(1)$ contribution can be integrated to obtain a solution for the pressure,

$$\tilde{p}^{(0)} = \frac{1}{2}\left(\frac{\partial\tilde{\Phi}^{(0)}}{\partial\xi}\right)^2, \qquad (51)$$

where the constant of integration has been set to zero using the far-field condition $\tilde{p}^{(0)} \to 0$ as $\xi \to \infty$. Thus, the pressure in the bath balances the normal component of the Maxwell stress, $\tilde{p}^{(0)} = \boldsymbol{n}\cdot\tilde{\mathbf{T}}_M^{(0)}\cdot\boldsymbol{n}$, and as a result $\tilde{\mathbf{T}}^{(0)}\cdot\boldsymbol{n} = 0$, implying that the normal stresses in the bath are $O(\beta^{-1})$ in size. This validates reducing the stress-continuity condition (28) to the stress-free condition on the gel (29).

The $O(\beta)$ problem involves the leading-order contribution to the viscous stress tensor, which is given by

$$\tilde{\mathbf{T}}_v^{(0)} = \mathcal{N}\left(\frac{\partial\tilde{\boldsymbol{v}}^{(0)}}{\partial\xi}\otimes\boldsymbol{n} + \boldsymbol{n}\otimes\frac{\partial\tilde{\boldsymbol{v}}^{(0)}}{\partial\xi}\right). \qquad (52)$$

Using the incompressibility condition (48), we find that

$$\tilde{\mathbf{T}}_v^{(0)}\cdot\boldsymbol{n} = \mathcal{N}\frac{\partial\tilde{\boldsymbol{v}}^{(0)}}{\partial\xi}. \qquad (53)$$

By using (51) and (53), the tangential components of the stress balance can be written as

$$\mathcal{N}\frac{\partial^2}{\partial\xi^2}\left(\tilde{\boldsymbol{v}}^{(0)}\cdot\boldsymbol{t}_i\right) + \frac{\partial^2\tilde{\Phi}^{(0)}}{\partial\xi^2}\nabla_s\tilde{\Phi}^{(0)}\cdot\boldsymbol{t}_i - \frac{\partial\tilde{\Phi}^{(0)}}{\partial\xi}\frac{\partial}{\partial\xi}\left(\nabla_s\tilde{\Phi}^{(0)}\cdot\boldsymbol{t}_i\right) = 0. \qquad (54a)$$

This equation has also been derived by Yariv [30]. In principle, it can be solved with the boundary conditions

$$\tilde{\boldsymbol{v}}_i^{(0)}\cdot\boldsymbol{t}_i\Big|_{\xi\to0^+} = U_i, \qquad \frac{\partial}{\partial\xi}\left(\tilde{\boldsymbol{v}}_i^{(0)}\cdot\boldsymbol{t}_i\right)\Big|_{\xi\to\infty} = 0, \qquad (54b)$$

where U_i can be computed from the mechanical problem for the gel.

Chemical potentials and fluxes Expanding the chemical potentials gives, to leading order,

$$\tilde{\mu}_s^{(0)} = \log\tilde{\phi}_s^{(0)} + \epsilon_r\tilde{p}^{(0)}, \qquad (55a)$$

$$\tilde{\mu}_\pm^{(0)} = \log\tilde{\phi}_\pm^{(0)} + \epsilon_r\tilde{p}^{(0)} + z_\pm\tilde{\Phi}^{(0)}. \qquad (55b)$$

The $O(\beta^{-1})$ contributions to the flux relation (17a) gives

$$\frac{\partial \tilde{\mu}_{\pm}^{(0)}}{\partial \xi} - \sum_{m \in \mathbb{M}} \tilde{\phi}_m^{(0)} \frac{\partial \tilde{\mu}_m^{(0)}}{\partial \xi} = 0. \tag{56}$$

The summation in this equation represents a local form of the Gibbs–Duhem relation and is equal to zero. To show this, we first calculate through substitution of (55) that

$$\sum_{m \in \mathbb{M}} \tilde{\phi}_m^{(0)} \frac{\partial \tilde{\mu}_m^{(0)}}{\partial \xi} = \epsilon_r \frac{\partial \tilde{p}^{(0)}}{\partial \xi} + \left(z_+ \tilde{\phi}_+^{(0)} + z_- \tilde{\phi}_-^{(0)} \right) \frac{\partial \tilde{\Phi}^{(0)}}{\partial \xi}. \tag{57}$$

Inserting the solution for the pressure (51) and making use of the leading-order part of the Poisson problem for the voltage,

$$-\epsilon_r \frac{\partial^2 \tilde{\Phi}^{(0)}}{\partial \xi^2} = z_+ \tilde{\phi}_+^{(0)} + z_- \tilde{\phi}_-^{(0)}, \tag{58}$$

results in the terms on the right-hand side of (57) cancelling out. Therefore, we obtain

$$\sum_{m \in \mathbb{M}} \tilde{\phi}_m^{(0)} \frac{\partial \tilde{\mu}_m^{(0)}}{\partial \xi} = 0. \tag{59}$$

From (56) and (59), we can deduce that the leading-order chemical potentials are uniform across the double layer, giving

$$\log \tilde{\phi}_{\pm}^{(0)} + \epsilon_r \tilde{p}^{(0)} + z_{\pm} \tilde{\Phi}^{(0)} = M_{\pm}(s_1, s_2, t) \tag{60a}$$

$$\log \tilde{\phi}_s^{(0)} + \epsilon_r \tilde{p}^{(0)} = M_s(s_1, s_2, t). \tag{60b}$$

By imposing the matching conditions $\tilde{\mu}_m^{(0)} \to \mu_m^{\text{bath}}$, $\tilde{\phi}_m^{(0)} \to \phi_m^{\text{bath}}$, $\tilde{p}^{(0)} \to 0$, and $\tilde{\Phi}^{(0)} \to \Phi^{\text{bath}}$ as $\xi \to \infty$, we obtain

$$M_{\pm}(s_1, s_2, t) = \mu_{\pm}^{\text{bath}} = \log \phi_{+}^{\text{bath}} + z_{\pm} \Phi^{\text{bath}}, \tag{61a}$$

$$M_s(s_1, s_2, t) = \mu_s^{\text{bath}} = \log \phi_s^{\text{bath}}. \tag{61b}$$

Equating (60a) with (61a) provides an expression for the ion fractions in the double layer,

$$\tilde{\phi}_{\pm}^{(0)} = \phi_{+}^{\text{bath}} \exp\left[z_{\pm} (\Phi^{\text{bath}} - \Phi^{(0)}) - \epsilon_r \tilde{p}^{(0)} \right]. \tag{62}$$

The electrical problem in the bath The leading-order problem electrical problem is obtained by combining (58) with the ionic volume fractions (62) to obtain a modified Poisson–Boltzmann equation given by

$$-\epsilon_r \frac{\partial^2 \tilde{\Phi}^{(0)}}{\partial \xi^2} = \exp\left[-(\epsilon_r/2)(\partial \tilde{\Phi}^{(0)}/\partial \xi)^2 \right] \sum_{i \in \mathbb{I}} z_i \phi_i^{\text{bath}} \exp\left(z_i (\Phi^{\text{bath}} - \tilde{\Phi}^{(0)}) \right), \tag{63}$$

where we have used (51) to eliminate the pressure. This equation can be integrated once and the conditions $\partial \tilde{\Phi}^{(0)}/\partial \xi \to 0$ and $\tilde{\Phi}^{(0)} \to \Phi^{\text{bath}}$ as $\xi \to \infty$ used to obtain

$$\frac{\partial \tilde{\Phi}^{(0)}}{\partial \xi} = \mp \sqrt{ \frac{2}{\epsilon_r} \log \left\{ 1 + \sum_{i \in \mathbb{I}} \phi_i^{\text{bath}} \left[\exp\left(z_i (\Phi^{\text{bath}} - \tilde{\Phi}^{(0)}) \right) - 1 \right] \right\} }. \tag{64}$$

The minus sign is taken if $\Phi^{\text{gel}} - \Phi^{\text{bath}} > 0$, which will generally be the case if the fixed charges on the polymer chains are positive, as assumed here.

3.2.2 Inner problem for the gel

Mass conservation Following the same approach as in the bath, the leading-order mass balance for the polymer network leads to

$$-\beta^{-1}V_n\frac{\partial\tilde{\phi}_n^{(0)}}{\partial\xi}+\beta^{-1}\frac{\partial}{\partial\xi}\left(\tilde{\phi}_n^{(0)}\tilde{\boldsymbol{v}}_n^{(0)}\cdot\boldsymbol{n}\right)=0 \tag{65}$$

Integrating and imposing the kinematic boundary condition (23) at the gel-bath interface ($\xi=0$) gives

$$\tilde{\boldsymbol{v}}_n^{(0)}\cdot\boldsymbol{n}=V_n. \tag{66}$$

Similarly, by expressing (6b) in inner coordinates, integrating the $O(\beta^{-1})$ contribution, and using (66), we find that the diffusive fluxes are uniform and given by

$$\tilde{\boldsymbol{j}}_m^{(0)}\cdot\boldsymbol{n}=A_m(s_1,s_2,t)=\boldsymbol{j}_m^{\text{gel}}\cdot\boldsymbol{n}. \tag{67}$$

where the A_m are the same as those appearing in (46) and (47) due to the boundary conditions (24). The second equality in (67) comes from matching to the outer solution.

Chemical potentials and fluxes The $O(\beta^{-1})$ contributions to the constitutive relations for the flux (8) give

$$\frac{\partial\tilde{\mu}_s^{(0)}}{\partial\xi}=0,\quad \frac{\partial\tilde{\mu}_\pm^{(0)}}{\partial\xi}=0, \tag{68}$$

implying the chemical potentials in the gel are also constant across the double layer. Thus, we have that

$$\tilde{\mu}_m^{(0)}(\xi,s_1,s_2,t)=M_m(s_1,s_2,t)=\mu_m^{\text{gel}}. \tag{69}$$

The $O(1)$ contributions to (8) provide expressions for the tangential components of the diffusive fluxes,

$$\tilde{\boldsymbol{j}}_s^{(0)}\cdot\boldsymbol{t}_i=-\mathcal{D}_s(\tilde{J}^{(0)})\sum_{m\in\mathbb{M}}\tilde{\phi}_m^{(0)}\,\nabla_s\mu_m^{\text{gel}}\cdot\boldsymbol{t}_i, \tag{70a}$$

$$\tilde{\boldsymbol{j}}_\pm^{(0)}\cdot\boldsymbol{t}_i=-\mathcal{D}_\pm\tilde{\phi}_\pm^{(0)}\nabla_s\mu_\pm^{\text{gel}}\cdot\boldsymbol{t}_i+\frac{\tilde{\phi}_\pm}{\tilde{\phi}_s^{(0)}}\tilde{\boldsymbol{j}}_s^{(0)}\cdot\boldsymbol{t}_i, \tag{70b}$$

which will be used in calculating the tangential mixture velocity; see (84).

The chemical potential of solvent can be expanded as

$$\begin{aligned}\tilde{\mu}_s^{(0)}=\tilde{\Pi}_s^{(0)}+\mathcal{G}\tilde{p}^{(0)}-\beta^{-2}\omega^2\Bigg[&\frac{\partial^2}{\partial\xi^2}\left(\tilde{\phi}_s^{(0)}+\beta\tilde{\phi}_s^{(1)}+\beta^2\tilde{\phi}_s^{(2)}\right)+2\beta\kappa\frac{\partial}{\partial\xi}\left(\tilde{\phi}_s^{(0)}+\beta\tilde{\phi}_s^{(1)}\right)\\&+\beta^2\nabla_s^2\tilde{\phi}_s^{(0)}-\beta^2(\kappa_i\kappa_i)\xi\frac{\partial\tilde{\phi}_s^{(0)}}{\partial\xi}\Bigg]+O(\beta).\end{aligned} \tag{71}$$

Similarly, the boundary condition at the gel-bath interface (27) can be expanded to give $\partial\tilde{\phi}_s^{(n)}/\partial\xi=0$ at $\xi=0$ for $n=0,1,2$. The $O(\beta^{-2})$ and $O(\beta^{-1})$ contributions to (71) along with the boundary and matching conditions conditions give

$$\tilde{\phi}_s^{(0)}(\xi,s_1,s_2,t)=\phi_s^{\text{gel}}(s_1,s_2,t),\quad \tilde{\phi}_s^{(1)}(\xi,s_1,s_2,t)=\phi_s^{(1)}(s_1,s_2,t), \tag{72}$$

which show that solvent concentration is uniform across the double layer to leading and next order. This is a consequence of the strong interfacial free energy, which effectively extends the variational condition (27) across the entire double layer. Using (72) in (71), we find that the solvent chemical potential simplifies to

$$\tilde{\mu}_s^{(0)}(\xi, s_1, s_2, t) = \tilde{\Pi}_s^{(0)} + \mathcal{G}\tilde{p}^{(0)} - \omega^2\left(\frac{\partial^2\tilde{\phi}_s^{(2)}}{\partial\xi^2} + \nabla_s^2\phi_s^{\mathsf{gel}}\right) = M_s(s_1, s_2, t). \tag{73}$$

By matching to the outer solution we find that

$$M_s(s_1, s_2, t) = \Pi_s^{\mathsf{gel}} + \mathcal{G}p^{\mathsf{gel}} - \omega^2\nabla^2\phi_s^{\mathsf{gel}}. \tag{74}$$

The chemical potentials of the ions can be expanded as

$$\tilde{\mu}_\pm^{(0)}(s_1, s_2, t) = \log\tilde{\phi}_\pm^{(0)} + \frac{1}{\tilde{J}^{(0)}}(1 - \chi\phi_s^{\mathsf{gel}}) + \mathcal{G}\tilde{p}^{(0)} + z_\pm\tilde{\Phi}^{(0)} = M_\pm(s_1, s_2, t), \tag{75}$$

where matching gives

$$M_\pm(s_1, s_2, t) = \log\phi_\pm^{\mathsf{gel}} + \frac{1}{J^{\mathsf{gel}}}(1 - \chi\phi_s^{\mathsf{gel}}) + \mathcal{G}p^{\mathsf{gel}} + z_\pm\Phi^{\mathsf{gel}}. \tag{76}$$

By combining (75) and (76) and using (72) we find that

$$\tilde{\phi}_\pm^{(0)} = \phi_\pm^{\mathsf{gel}}\exp\left[z_\pm(\Phi^{\mathsf{gel}} - \tilde{\Phi}^{(0)}) + \mathcal{G}(p^{\mathsf{gel}} - \tilde{p}^{(0)}) + \left(\frac{1}{J^{\mathsf{gel}}} - \frac{1}{\tilde{J}^{(0)}}\right)(1 - \chi\phi_s^{\mathsf{gel}})\right]. \tag{77}$$

Although this appears to be a closed-form expression for the volume fraction of ions, it is important to recall that the Jacobian determinant J also depends on the these quantities; see (4).

Kinematics Expanding the relation $\boldsymbol{X} = \boldsymbol{x} - \boldsymbol{a}$ in terms of inner variables gives

$$\tilde{\boldsymbol{X}}^{(0)} = \boldsymbol{r} - \tilde{\boldsymbol{a}}^{(0)}, \tag{78a}$$

$$\tilde{\boldsymbol{X}}^{(1)} = \xi\boldsymbol{n} - \tilde{\boldsymbol{a}}^{(1)}. \tag{78b}$$

The $O(\beta^{-1})$ contribution to (2) implies that $\tilde{\boldsymbol{X}}^{(0)} \otimes \boldsymbol{n}$ is constant across the double layer. Multiplying by $\boldsymbol{n}$ and matching to the outer solution gives $\tilde{\boldsymbol{X}}^{(0)} = \boldsymbol{X}^{\mathsf{gel}} = \boldsymbol{r} - \boldsymbol{a}^{\mathsf{gel}}$, which implies from (78a) that $\tilde{\boldsymbol{a}}^{(0)} = \boldsymbol{a}^{\mathsf{gel}}$. The $O(1)$ contribution to (2) then gives

$$\tilde{\mathbf{F}}^{(0)} = \left(\frac{\partial\tilde{\boldsymbol{X}}^{(1)}}{\partial\xi} \otimes \boldsymbol{n} + \nabla_s\boldsymbol{X}^{\mathsf{gel}}\right)^{-1}, \tag{79}$$

The Jacobian can be linked to the displacement via the condition

$$\frac{1}{\tilde{J}^{(0)}} = \det\left(\frac{\partial\tilde{\boldsymbol{X}}^{(1)}}{\partial\xi} \otimes \boldsymbol{n} + \nabla_s\boldsymbol{X}^{\mathsf{gel}}\right), \tag{80}$$

which we interpret as providing an expression for the normal component of $\tilde{\boldsymbol{X}}^{(1)}$. The tangential components of $\tilde{\boldsymbol{X}}^{(1)}$ are determined by tangential stress balances, as discussed below.

Momentum conservation Due to the difference in how the equations for the bath and gel are non-dimensionalised, there is no need to introduce a further rescaling of the pressure and stress tensors for the inner gel problem. The leading-order part of the stress balance in the gel (12), expressed in inner coordinates, is

$$\frac{\partial}{\partial\xi}\left(\tilde{\mathsf{T}}^{(0)}\cdot\boldsymbol{n}\right) = 0. \tag{81}$$

Thus, by integrating (81) and imposing the simplified boundary condition (29), we find that

$$\tilde{\mathsf{T}}^{(0)}\cdot\boldsymbol{n} = \tilde{\mathsf{T}}_e^{(0)}\cdot\boldsymbol{n} + \tilde{\mathsf{T}}_M^{(0)}\cdot\boldsymbol{n} + \tilde{\mathsf{T}}_K^{(0)}\cdot\boldsymbol{n} - \tilde{p}^{(0)}\boldsymbol{n} = 0 \tag{82}$$

across the double layer. The leading-order Maxwell and Korteweg stress tensors are

$$\tilde{\mathsf{T}}_M^{(0)} = \frac{1}{\mathcal{G}}\left(\frac{\partial\tilde{\Phi}^{(0)}}{\partial\xi}\right)^2\left(\boldsymbol{n}\otimes\boldsymbol{n} - \frac{1}{2}\mathsf{I}\right), \tag{83a}$$

$$\tilde{\mathsf{T}}_K^{(0)} = \frac{\omega^2}{\mathcal{G}}\left\{\left[\frac{1}{2}|\nabla\phi_s^{\mathsf{gel}}|^2 + \phi_s^{\mathsf{gel}}\left(\frac{\partial^2\tilde{\phi}_s^{(2)}}{\partial\xi^2} + \nabla_s^2\phi_s^{\mathsf{gel}}\right)\right]\mathsf{I} - \nabla_s\phi_s^{\mathsf{gel}}\otimes\nabla_s\phi_s^{\mathsf{gel}}\right\}. \tag{83b}$$

Since $\boldsymbol{t}_i\cdot\tilde{\mathsf{T}}_M^{(0)}\cdot\boldsymbol{n} = 0$ and $\boldsymbol{t}_i\cdot\tilde{\mathsf{T}}_K^{(0)}\cdot\boldsymbol{n} = 0$, the tangential component of (82) implies that $\boldsymbol{t}_i\cdot\tilde{\mathsf{T}}_e^{(0)}\cdot\boldsymbol{n} = 0$, which can be formulated as a problem for the tangential components of $\tilde{\boldsymbol{X}}^{(1)}$. Having, in principle, determined the three components of $\tilde{\boldsymbol{X}}^{(1)}$ from the two tangential stress conditions and evaluating the determinant (80), the deformation gradient tensor $\tilde{\mathsf{F}}^{(0)}$ is now fully specified. This allows the tangential component of the mixture velocity to be evaluated using (7) and (5) as

$$\tilde{\boldsymbol{v}}^{(0)}\cdot\boldsymbol{t}_i = \boldsymbol{t}_i\cdot\tilde{\mathsf{F}}^{(0)}\cdot\frac{\partial\boldsymbol{a}^{\mathsf{gel}}}{\partial t} + \sum_{m\in\mathbb{M}}\tilde{\boldsymbol{j}}_m^{(0)}\cdot\boldsymbol{t}_i, \tag{84}$$

where the tangential components of the flux are given by (70). Taking the limit of (84) as $\xi\to 0^-$ enables the quantity U_i in (54b) to be determined.

The normal component of (82) implies that

$$\tilde{p}^{(0)} = \boldsymbol{n}\cdot\left(\tilde{\mathsf{T}}_e^{(0)} + \tilde{\mathsf{T}}_K^{(0)} + \tilde{\mathsf{T}}_M^{(0)}\right)\cdot\boldsymbol{n}. \tag{85}$$

In order to evaluate the Korteweg stresses without explicitly solving for $\tilde{\phi}_s^{(2)}$, the expression for the solvent chemical potential (73) can be used in (83b) to obtain

$$\boldsymbol{n}\cdot\tilde{\mathsf{T}}_K^{(0)}\cdot\boldsymbol{n} = \frac{1}{\mathcal{G}}\left[\frac{\omega^2}{2}|\nabla\phi_s^{\mathsf{gel}}|^2 + \phi_s^{\mathsf{gel}}\left(\tilde{\Pi}_s^{(0)} - M_s\right)\right] + \phi_s^{\mathsf{gel}}\tilde{p}^{(0)}. \tag{86}$$

where M_s is given by (74). Setting $\omega = 0$ leads to $\boldsymbol{n}\cdot\tilde{\mathsf{T}}_K^{(0)}\cdot\boldsymbol{n} = 0$ because $\tilde{\Pi}_s^{(0)} + \mathcal{G}\tilde{p}^{(0)} - M_s = 0$ from (73). Substitution of (86) into (85) gives an algebraic relation for the pressure $\tilde{p}^{(0)}$.

The electrical problem in the gel The leading-order electrical problem in the gel is given by

$$-\frac{\partial^2\tilde{\Phi}^{(0)}}{\partial\xi^2} = z_+\tilde{\phi}_+^{(0)} + z_-\tilde{\phi}_-^{(0)} + z_f\tilde{\phi}_f^{(0)}, \tag{87}$$

which is coupled to the algebraic equations for the volume fractions of ions (77) and the mechanical pressure (85). The electrical problems for the bath and gel can be decoupled by combining the first integral for the electric potential in the bath (64) with the electrostatic boundary conditions $\tilde{\Phi}^{(0)}(0^-, s_1, s_2, t) = \tilde{\Phi}^{(0)}(0^+, s_1, s_2, t)$ and $\partial_\xi \tilde{\Phi}^{(0)}(0^-, s_1, s_2, t) = \epsilon_r \partial_\xi \tilde{\Phi}^{(0)}(0^+, s_1, s_2, t)$ to obtain

$$\left.\frac{\partial \tilde{\Phi}^{(0)}}{\partial \xi}\right|_{\xi=0^-} = \mp \sqrt{2\epsilon_r \log\left\{1 + \sum_{i\in\mathbb{I}} \phi_i^{\text{bath}} \left[\exp\left(z_i(\Phi^{\text{bath}} - \tilde{\Phi}^{(0)})\right) - 1\right]\right\}}, \tag{88}$$

which acts as a boundary condition for (87). The electrical problem in the gel is closed by imposing the matching condition $\tilde{\Phi}^{(0)} \to \Phi^{\text{gel}}$ as $\xi \to -\infty$.

3.3 Matching: effective jump conditions across the gel-bath interface

We now derive boundary conditions for the electroneutral model by connecting the outer solutions in the bath and gel to each through matching to the inner solutions and imposing the boundary conditions at the gel-bath interface.

Kinematic conditions By imposing mass conservation at the gel-bath interface (23), we can equate (47) with (67) to obtain

$$\dot{\boldsymbol{j}}_m^{\text{gel}} \cdot \boldsymbol{n} = \boldsymbol{q}_m^{\text{bath}} \cdot \boldsymbol{n} + \phi_m^{\text{bath}}(\boldsymbol{v}^{\text{bath}} \cdot \boldsymbol{n} - V_n). \tag{89}$$

Moreover, by matching (66) to the solution as $\xi \to -\infty$, the outer problem obeys the usual kinematic boundary condition on the network

$$\boldsymbol{v}_n^{\text{gel}} \cdot \boldsymbol{n} - V_n = 0. \tag{90}$$

By summing (89) over $m \in \mathbb{M}$, the mixture velocities are found to satisfy

$$\boldsymbol{v}^{\text{gel}} \cdot \boldsymbol{n} = \boldsymbol{v}^{\text{bath}} \cdot \boldsymbol{n}. \tag{91}$$

Assuming the anion fraction is eliminated from the outer problems, then only the jump conditions in (89) for the solvent and cation need to be imposed. However, the jump conditions for the ions can be combined to obtain

$$(z_+ \dot{\boldsymbol{j}}_+^{\text{gel}} + z_- \dot{\boldsymbol{j}}_-^{\text{gel}}) \cdot \boldsymbol{n} = (z_+ \boldsymbol{q}_+^{\text{bath}} + z_- \boldsymbol{q}_-^{\text{bath}}) \cdot \boldsymbol{n}, \tag{92}$$

which provides a condition on the normal derivatives of the electric potential.

Continuity of chemical potentials By combining (26) along with (61) and (69), continuity of chemical potential across the interface is recovered: $\mu_m^{\text{gel}} = \mu_m^{\text{bath}}$. Continuity of the solvent chemical potential means that (74) can be equated with (61b) to produce

$$\Pi_s^{\text{gel}} + \mathcal{G}p^{\text{gel}} - \omega^2 \nabla^2 \phi_s^{\text{gel}} = \log \phi_s^{\text{bath}}. \tag{93}$$

Equating the chemical potentials of the ions, i.e. (61a) with (76), provides a jump condition for the ionic volume fractions

$$\phi_\pm^{\text{gel}} = \phi_\pm^{\text{bath}} \exp\left[z_\pm(\Phi^{\text{bath}} - \Phi^{\text{gel}}) - \mathcal{G}p^{\text{gel}} - \frac{1}{J^{\text{gel}}}(1 - \chi\phi_s^{\text{gel}})\right]. \tag{94}$$

Using (94) in the electroneutrality condition for the gel (37) produces a jump condition for the electrical potentials

$$\sum_{i\in\mathbb{I}} z_i\phi_i^{\text{bath}} \exp\left(z_i(\Phi^{\text{bath}} - \Phi^{\text{gel}})\right) = z_f\phi_f \exp\left[\mathcal{G}p^{\text{gel}} + \frac{1}{J^{\text{gel}}}(1-\chi\phi_s^{\text{gel}})\right]. \tag{95}$$

These equations are also coupled to the molecular incompressibility condition in the gel (4), the no-void condition in the bath (16), and the elecroneutrality condition in the bath (32).

Variational condition Matching the derivatives of the solvent fraction in the gel using (72) recovers the variational condition

$$\nabla\phi_s^{\text{gel}} \cdot \boldsymbol{n} = 0. \tag{96}$$

Continuity of stress By matching (82) with the outer solution, we obtain stress-free conditions for the gel at the interface:

$$\mathsf{T}^{\text{gel}} \cdot \boldsymbol{n} = 0. \tag{97}$$

Slip condition The final boundary condition for the electroneutral model is a slip condition on the mixture velocity of the bath. This is obtained by solving (54) using the value of U_i from the gel problem (84) and then imposing the matching conditions $\tilde{\boldsymbol{v}}^{(0)} \cdot \boldsymbol{t}_i \to \boldsymbol{v}^{\text{bath}} \cdot \boldsymbol{t}_i$ as $\xi \to \infty$.

4 Analysis without interfacial free energy

The asymptotic analysis of the inner region is slightly different for models that neglect the interfacial free energy and take $\omega = 0$. The lack of a non-local term in the solvent chemical potential in the gel gives rise to gradients in the solvent fraction across the double layer. From (71), the leading-order contribution to μ_s in the double layer now becomes

$$\tilde{\mu}_s^{(0)} = \tilde{\Pi}_s^{(0)} + \mathcal{G}\tilde{p}^{(0)} = \mu_s^{\text{gel}}, \tag{98a}$$

which can be interpreted as a nonlinear algebraic equation for $\tilde{\phi}_s^{(0)} = \phi_s^{(0)}(\xi, s_1, s_2, t)$. The corresponding ion fractions are given by

$$\tilde{\phi}_\pm^{(0)} = \phi_\pm^{\text{gel}} \exp\left[z_\pm(\Phi^{\text{gel}} - \tilde{\Phi}^{(0)}) + \mathcal{G}(p^{\text{gel}} - \tilde{p}^{(0)}) + \frac{1-\chi\phi_s^{\text{gel}}}{J^{\text{gel}}} - \frac{1-\chi\tilde{\phi}_s^{(0)}}{\tilde{J}^{(0)}}\right]. \tag{98b}$$

The pressure in the gel across the double layer can be calculated directly from (85) after neglecting the Korteweg stresses. The matching conditions across the double layer are the same as those in Sec. 3.3 except the non-local term in (93) and the variational condition in (96) can be dropped.

5 Specialisation to plane-strain problems

The asymptotic analysis can be further developed by considering plane-strain problems, e.g. those involving cylindrical geometries with arbitrary cross sections, as shown in Fig. 2. We assume that the

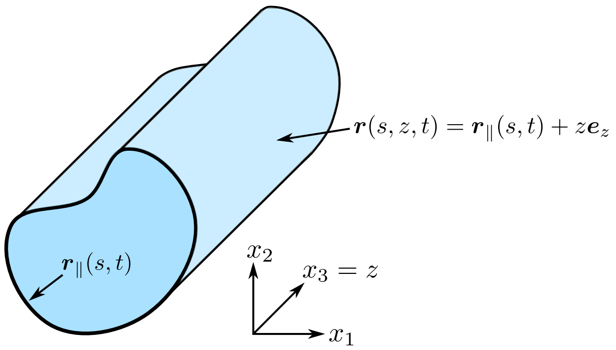

Figure 2: The geometry of a cylindrical hydrogel. The quantity $\boldsymbol{r}_{\|}$ represents the one-dimensional gel-bath interface formed at each cross section and is parametrised by its arclength s. The two-dimensional gel-bath interface $\boldsymbol{r}$ is parametrised in terms of s and the axial coordinate z. The coordinates x_1 and x_2 lie in the cross-sectional plane.

unit vectors $\boldsymbol{e}_1$ and $\boldsymbol{e}_2$ span the cross-sectional plane and that $\boldsymbol{e}_3$ is aligned with the axial direction, which we also denote by $\boldsymbol{e}_z$ for simplicity. Similarly, we let $z \equiv x_3$ denote the axial coordinate. Using this construction, any vector $\boldsymbol{u}$ can be decomposed into components $\boldsymbol{u}_{\|}$ and u_z that lie in the cross-sectional plane and in the axial direction according to $\boldsymbol{u} = \boldsymbol{u}_{\|} + u_z\boldsymbol{e}_z$, with $\boldsymbol{u}_{\|} = u_\alpha \boldsymbol{e}_\alpha$, where we adopt the convention that Greek indices are equal to 1 or 2.

The plane-strain problem is formulated by writing the deformation gradient tensor as $\mathsf{F}(\boldsymbol{x},t) = \mathsf{F}_{\|}(\boldsymbol{x}_{\|},t) + \lambda_z \boldsymbol{e}_z \otimes \boldsymbol{E}_z$, where $\mathsf{F}_{\|} = \nabla_{\|}\boldsymbol{X}_{\|}$, $\boldsymbol{X}_{\|} = X_\alpha(\boldsymbol{x}_{\|},t)\boldsymbol{E}_\alpha$, and λ_z corresponds to a constant stretch or compression that is imposed in the axial direction. The corresponding displacement is written as $\boldsymbol{a} = \boldsymbol{a}_{\|}(\boldsymbol{x}_{\|},t) + a_z(z,t)\boldsymbol{E}_z$. From (3) it follows that $\mathsf{F}_{\|} = (\mathsf{I}_{\|} - \nabla_{\|}\boldsymbol{a}_{\|})^{-1}$ and $\lambda_z = (1 - \partial a_z/\partial z)^{-1}$. Similarly, the Jacobian can be decomposed as $J = J_{\|}\lambda_z$ where $J_{\|} = \det \mathsf{F}_{\|}$. We assume that all variables, except for a_z, are independent of the axial coordinate z.

The outer problem is trivially to formulate and will not be discussed in detail. Instead, we focus on the inner problem for the solid mechanics of the gel. The gel-bath interface can be parametrised in terms of $s_1 = s$ and $s_2 = z$ as $\boldsymbol{r}(s_1, s_2, t) = \boldsymbol{r}_{\|}(s,t) + z\boldsymbol{e}_z$. The quantity $\boldsymbol{r}_{\|}$ represents the one-dimensional gel-bath interface formed at each cross section, which is parameterised in terms of its arclength s. The corresponding *unit* tangent vectors are $\boldsymbol{t}_1 = \partial \boldsymbol{r}_{\|}/\partial s \equiv \boldsymbol{t}$ and $\boldsymbol{t}_2 = \boldsymbol{e}_z$ and satisfy $\boldsymbol{t} \cdot \boldsymbol{e}_z = 0$. The triad $\{\boldsymbol{t}, \boldsymbol{e}_z, \boldsymbol{n}\}$ thus forms an orthonormal basis. From the calculations in Appendix C, it follows that the principal curvatures of the surface are given by κ_1 and $\kappa_2 = 0$ and the derivatives in the inner region transform according to (43) with $\nabla_s = \boldsymbol{t}\,\partial_s + \boldsymbol{e}_z \partial_z$ and $\nabla_s^2 = \partial_{ss} + \partial_{zz}$.

It is convenient to introduce the Lagrangian analogues of the gel-bath interface $\boldsymbol{r}_{\|}$, its arclength s, and the normal and tangent vectors $\boldsymbol{n}$ and $\boldsymbol{t}$; these are denoted by $\boldsymbol{R}_{\|}$, S, $\boldsymbol{N}$, and $\boldsymbol{T} = \partial_S \boldsymbol{R}_{\|}$, respectively. We also introduce the Lagrangian normal coordinate Ξ, which is analogous to ξ; see (42). Using these quantities, we write the Lagrangian coordinates in terms of interfacial quantities according to $\boldsymbol{X}_{\|}(S, \Xi, t) = \boldsymbol{R}_{\|}(S,t) + \beta\Xi\boldsymbol{N}(S,t)$. The in-plane deformation gradient tensor in inner coordinates can be calculated by writing $S = \tilde{S}(s,\xi,t)$ and $\Xi = \tilde{\Xi}(s,\xi,t)$ to find

$$\left[\tilde{\mathsf{F}}_{\|}^{(0)}\right]^{-1} = \beta^{-1}\frac{\partial \tilde{S}}{\partial \xi}\boldsymbol{T} \otimes \boldsymbol{n} + \frac{\partial \tilde{\Xi}}{\partial \xi}\boldsymbol{N} \otimes \boldsymbol{n} + \tilde{\Xi}\frac{\partial \tilde{S}}{\partial \xi}\frac{\partial \boldsymbol{N}}{\partial S} \otimes \boldsymbol{n} + \frac{\partial \tilde{S}}{\partial s}\boldsymbol{T} \otimes \boldsymbol{t} + O(\beta). \tag{99}$$

We now asymptotically expand the Lagrangian coordinates as $\tilde{S} = \tilde{S}^{(0)} + \beta\tilde{S}^{(1)} + O(\beta^2)$ and $\Xi = \tilde{\Xi}^{(1)} + O(1)$. The $O(\beta^{-1})$ contributions to (99) imply that $\partial_\xi \tilde{S}^{(0)} = 0$. By differentiating this expression with respect to the Eulerian coordinate s, we find that the tangential stretch, $\tilde{\lambda}_s^{(0)} = (\partial_s \tilde{S}^{(0)})^{-1}$, is uniform across the double layer. Thus, by matching to the outer solution, we can deduce that $\partial_s \tilde{S}^{(0)} = (\lambda_s^{\text{gel}})^{-1}$. The $O(1)$ contributions to (99) can be inverted to obtain a closed-form expression for the in-plane deformation gradient tensor,

$$\tilde{\mathsf{F}}_{\parallel}^{(0)} = \left(\frac{\partial \tilde{\Xi}^{(0)}}{\partial \xi}\right)^{-1} \boldsymbol{n} \otimes \boldsymbol{N} - \tilde{J}_{\parallel}^{(0)} \frac{\partial \tilde{S}^{(1)}}{\partial \xi} \boldsymbol{n} \otimes \boldsymbol{T} + \lambda_s^{\mathsf{gel}} \boldsymbol{t} \otimes \boldsymbol{T}, \tag{100}$$

where the in-plane determinant is given by

$$\tilde{J}_{\parallel}^{(0)} = \left(\frac{\partial \tilde{\Xi}^{(0)}}{\partial \xi}\right)^{-1} \lambda_s^{\mathsf{gel}}, \tag{101}$$

which provides an expression for $\tilde{\Xi}^{(0)}$. The in-plane components of the elastic stress tensor are

$$\tilde{\mathsf{T}}_{e,\parallel}^{(0)} = \frac{1}{\tilde{J}^{(0)}} \left(\tilde{\mathsf{B}}_{\parallel}^{(0)} - \boldsymbol{n} \otimes \boldsymbol{n} - \boldsymbol{t} \otimes \boldsymbol{t}\right). \tag{102}$$

Since the tangential components of the elastic stress vanish across the double layer, we have that $\boldsymbol{t} \cdot \tilde{\mathsf{B}}_{\parallel}^{(0)} \cdot \boldsymbol{n} = 0$, which leads to $\partial_\xi \tilde{S}^{(1)} = 0$. Thus, the in-plane deformation tensor (100) becomes diagonal, meaning that material elements undergo normal and tangential stretching without being sheared. The in-plane normal component of the elastic stress tensor, $\boldsymbol{n} \cdot \tilde{\mathsf{T}}_{e,\parallel}^{(0)} \cdot \boldsymbol{n}$, can be readily calculated and used to evaluate the pressure.

6 Swelling of a constrained cylinder

We now use our formulation to study electric double layers in swollen hydrogel cylinders that are free to swell in the radial direction but confined in the axial direction. This situation is motivated by the experimental setup considered by Horkay *et al.* [14]. We consider axisymmetric equilibrium solutions and let

$$\mathsf{F} = \lambda_r \, \boldsymbol{e}_r \otimes \boldsymbol{E}_R + \lambda_\theta \, \boldsymbol{e}_\theta \otimes \boldsymbol{E}_\Theta + \lambda_z \boldsymbol{e}_z \otimes \boldsymbol{E}_Z, \tag{103}$$

where λ_z is an experimentally controlled constant. The corresponding displacement vector has the form $\boldsymbol{a} = a_r \boldsymbol{E}_R + a_z \boldsymbol{E}_Z$, where a_r is the radial component. We restrict our attention to monovalent salts with $z_\pm = \pm 1$. The bath that surrounds the hydrogel is assumed to have a uniform composition and electric potential. The electroneutrality condition in the bath becomes $\phi_s^{\mathsf{bath}} = 1 - 2\phi_+^{\mathsf{bath}}$. The cation fraction, ϕ_+^{bath}, is treated as a free parameter. The electric potential, Φ^{bath}, is treated as an arbitrary constant, which we assume is non-zero for generality. We first formulate the outer problem in the gel and show that it reduces to a set of nonlinear algebraic equations for homogeneously swollen states that are in equilibrium with the bath. We then numerically solve the associated inner problems for models that account for and neglect interfacial free energy, and pay particular attention to the generation of hoop stresses across the Debye layer.

6.1 Solution of the outer problem: homogeneous equilibria

At equilibrium, the chemical potentials in the hydrogel must be spatially uniform, leading to $\mu_m = \mu_m^{\mathsf{gel}}$ for $m \in \mathbb{M}$. We assume that the outer solution corresponds to a homogeneously swollen cylindrical gel, in which case $\phi_m = \phi_m^{\mathsf{gel}}$ for $m \in \mathbb{M}$, $\lambda_\theta = \lambda_r = \lambda_r^{\mathsf{gel}}$, and $\mathsf{T}_{e,\theta\theta} = \mathsf{T}_{e,rr} = \mathsf{T}_{e,rr}^{\mathsf{gel}}$. The radial component of the elastic stress is given by $\mathsf{T}_{e,rr}^{\mathsf{gel}} = \lambda_z^{-1} - (J^{\mathsf{gel}})^{-1}$. The stress balance in the hydrogel reduces to $\partial p/\partial r = 0$. Imposing the matching condition (97) reveals that the fluid pressure balances the radial elastic stress, $p^{\text{gel}} = \mathsf{T}^{\text{gel}}_{e,rr}$. The volume fraction of solvent and ions, as well as the electric potential, are determined from the matching conditions

$$\log \phi_s^{\text{gel}} + \frac{1}{J^{\text{gel}}} + \frac{\chi(1-\phi_s^{\text{gel}})}{J^{\text{gel}}} + \mathcal{G}\left(\frac{1}{\lambda_z} - \frac{1}{J^{\text{gel}}}\right) = \log(1 - 2\phi_+^{\text{bath}}), \tag{104a}$$

$$\phi_\pm^{\text{gel}} = \phi_+^{\text{bath}} \exp\left[\pm(\Phi^{\text{bath}} - \Phi^{\text{gel}}) - \mathcal{G}\left(\frac{1}{\lambda_z} - \frac{1}{J^{\text{gel}}}\right) - \frac{1}{J^{\text{gel}}}\left(1 - \chi\phi_s^{\text{gel}}\right)\right], \tag{104b}$$

$$2\phi_+^{\text{bath}} \sinh(\Phi^{\text{bath}} - \Phi^{\text{gel}}) = -z_f\phi_f \exp\left[\mathcal{G}\left(\frac{1}{\lambda_z} - \frac{1}{J^{\text{gel}}}\right) + \frac{1}{J^{\text{gel}}}\left(1 - \chi\phi_s^{\text{gel}}\right)\right], \tag{104c}$$

where $\phi_f = C_f/J^{\text{gel}}$ and J^{gel} is given by (4).

We numerically solve the nonlinear system of algebraic equations defining the outer problem (i.e. the homogeneous equilibria) given by (104) using pseudo-arclength continuation. The results are shown as solid curves in Fig. 3 for three different values of $\lambda_z \leq 1$, corresponding to gels in axial compression. There are two distinct solution branches, one of which describes highly swollen gels ($J^{\text{gel}} > 10$), whereas the other corresponds to weakly swollen gels ($J^{\text{gel}} \sim 1.4$). We refer to the former and latter as the swollen and collapsed branches, respectively. These two branches indicate that a volume phase transition occurs a critical salt concentration ϕ_+^{bath}. Increasing the axial compression reduces the degree of swelling for a given salt fraction as well as the critical salt fraction at which the volume phase transition occurs, both of which agree with experimental observations [14]. Due to the incompressibility of the gel, imposing an axial compression results in a radial stretch. The elasticitic energy cost of this radial 'pre-stretch' means that fewer solvent molecules can be inserted into the gel before the energy decrease due to mixing is balanced by the energy increase of further radial stretching. Hence, the equilibrium swelling ratio J^{gel} decreases with the axial stretch λ_z.

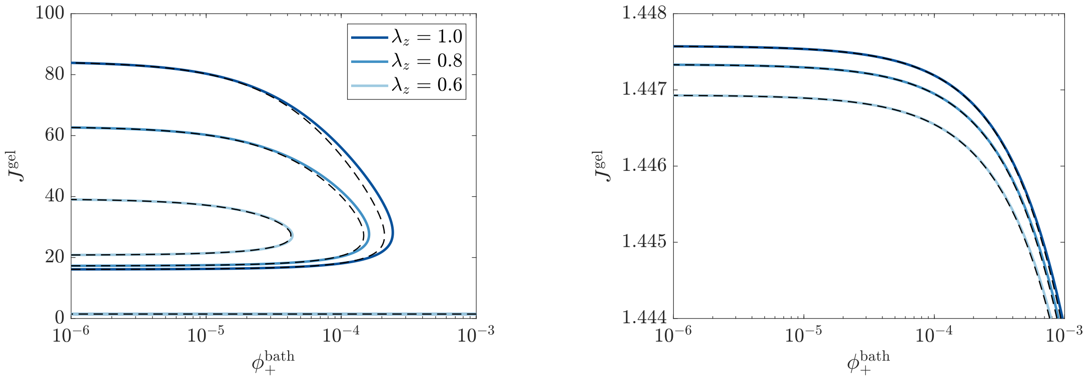

(a) **(b)**

Figure 3: Equilibrium swelling ratio J^{gel} as a function of cation fraction in the bath ϕ_+^{bath}. Panel (b) focuses on the collapsed branch. Solid and dashed lines correspond to numerical solutions of (104) and the reduced equation (108), respectively. The parameter values are $\mathcal{G} = 0.0005$, $\chi = 1.2$, $C_f = 0.05$ $z_\pm = \pm 1$, $z_f = 1$.

The nonlinear system for the outer solution (104) can be greatly simplified in the limit of a dilute salt, $\phi_+^{\text{bath}} \ll \phi_f$. Balancing terms in the electroneutrality condition (104c) gives

$$\Phi^{\text{gel}} - \Phi^{\text{bath}} \sim \log\left(\frac{z_f\phi_f}{\phi_+^{\text{bath}}}\right) + \mathcal{G}\left(\frac{1}{\lambda_z} - \frac{1}{J^{\text{gel}}}\right) + \frac{1}{J^{\text{gel}}}(1 - \chi\phi_s^{\text{gel}}), \tag{105}$$

where we have assumed that $\mathcal{G}/J^{\text{gel}}$ at most $O(1)$ in size. The ion fractions in the gel are approximately given by

$$\phi_+^{\mathsf{gel}} \sim \frac{(\phi_+^{\mathsf{bath}})^2}{z_f \phi_f} \exp\left[-2\mathcal{G}\left(\frac{1}{\lambda_z} - \frac{1}{J^{\mathsf{gel}}}\right) - \frac{2}{J^{\mathsf{gel}}}(1 - \chi\phi_s^{\mathsf{gel}})\right], \qquad \phi_-^{\mathsf{gel}} \sim z_f \phi_f, \tag{106}$$

showing that the anions, to leading order in ϕ_+^{bath}, balance the fixed charges on the polymer chains. Since the cation fraction ϕ_+^{gel} will be extremely small relative to the anion fraction ϕ_-^{gel}, the Jacobian determinant then reduces to

$$J^{\mathsf{gel}} \sim \frac{1 + z_f C_f}{1 - \phi_s^{\mathsf{gel}}}, \tag{107}$$

where we have used $\phi_f = C_f / J^{\mathsf{gel}}$. The solvent fraction can then be obtained by solving

$$\log \phi_s^{\mathsf{gel}} + \frac{1 - \phi_s^{\mathsf{gel}}}{1 + z_f C_f} + \frac{\chi(1 - \phi_s^{\mathsf{gel}})^2}{1 + z_f C_f} + \mathcal{G}\left(\frac{1}{\lambda_z} - \frac{1 - \phi_s^{\mathsf{gel}}}{1 + z_f C_f}\right) = -2\phi_+^{\mathsf{bath}}, \tag{108}$$

and used to evaluate the Jacobian determinant, ion fractions, and jump in electric potential. The black dashed lines in Fig. 3 represent solutions of (108), which are in very good agreement with the full nonlinear system (104).

6.2 Solution of the inner problem

The inner problem consists of a differential-algebraic system involving the Poisson–Boltzmann equation for the electric potential in the gel (87) along with coupled algebraic relations for the volume fractions of the solvent and ions. Once the inner problem in the gel is solved, the electrical potential in the bath can be obtained by integrating (64). The electrical and mechanical problems in the gel are coupled through the appearance of the pressure in the ion distributions (77) or (98b). To formulate the mechanical problem, we must first account for non-homogeneous deformations that occur across the double layer due to composition gradients. Thus, the in-plane components of the deformation gradient (103) are expanded as $\tilde{\mathbf{F}}_{\parallel}^{(0)} = \tilde{\lambda}_r^{(0)} \boldsymbol{n} \otimes \boldsymbol{N} + \tilde{\lambda}_\theta^{(0)} \boldsymbol{t} \otimes \boldsymbol{T}$. By comparing this expansion with (100) and using $\lambda_s^{\mathsf{gel}} = \lambda_r^{\mathsf{gel}} = (J^{\mathsf{gel}}/\lambda_z)^{1/2}$, we can deduce that

$$\tilde{\mathbf{F}}_{\parallel}^{(0)} = \tilde{J}^{(0)} \left(\frac{1}{\lambda_z J^{\mathsf{gel}}}\right)^{1/2} \boldsymbol{n} \otimes \boldsymbol{N} + \left(\frac{J^{\mathsf{gel}}}{\lambda_z}\right)^{1/2} \boldsymbol{t} \otimes \boldsymbol{T}, \tag{109}$$

The radial elastic stress can be calculated from (102) as

$$\tilde{\mathsf{T}}_{e,rr}^{(0)} = \boldsymbol{n} \cdot \tilde{\mathbf{T}}_{e,\parallel} \cdot \boldsymbol{n} = \frac{1}{\lambda_z} \frac{\tilde{J}^{(0)}}{J^{\mathsf{gel}}} - \frac{1}{\tilde{J}^{(0)}}, \tag{110}$$

which allows the pressure to be determined from (85). Moreover, the expression for the hoop stress in the hydrogel, $\tilde{\mathsf{T}}_{\theta\theta}^{(0)} = \boldsymbol{t} \cdot \tilde{\mathbf{T}}^{(0)} \cdot \boldsymbol{t}$, is the same in the $\omega = 0$ and $\omega \gg \beta$ cases:

$$\tilde{\mathsf{T}}_{\theta\theta}^{(0)} = \frac{1}{\lambda_z}\left(\frac{J^{\mathsf{gel}}}{\tilde{J}^{(0)}} - \frac{\tilde{J}^{(0)}}{J^{\mathsf{gel}}}\right) - \mathcal{G}^{-1}\left(\frac{\partial \tilde{\Phi}^{(0)}}{\partial \xi}\right)^2. \tag{111}$$

The first term represents the elastic contribution to the total hoop stress, which can be compressive or tensile. The second term captures the contribution from the Maxwell stresses, which is always compressive. The nonlinear differential-algebraic system for the electric potential and volume fractions in the gel is discretised using finite differences and solved using Newton's method.

We first consider the case when $\lambda_z = 1.0$, $\phi_+^{\text{bath}} = 10^{-5}$, with the remaining parameters being the same as those in Fig. 3. Thus, there are three possible solutions to the outer problem. We are only concerned with two of these, which correspond to the collapsed state ($J^{\text{gel}} \simeq 1.447$) and the highly swollen state ($J^{\text{gel}} \simeq 82$). The other solution, which has a swelling ratio $J^{\text{gel}} \simeq 60$, is expected to be unstable [4]. The numerical solutions of the inner problems when the outer solution corresponds to the collapsed and swollen states are shown in Figs. 4 and 5, respectively. Solid and dashed lines denote models with and without interfacial free energy.

The results in Fig. 4 indicate that our non-dimensionalisation underestimates the width of the double layer, which is about 10β in the gel (or 1 nm) and 1000β in the bath (or 100 nm). Despite this underestimation, the gradient in the electric potential is strong enough to produce substantial Maxwell stresses, which act in conjunction with the Korteweg stresses to generate a large pressure in the gel. Due to the inclusion of interfacial free energy, the solvent fraction remains uniform across the double layer, effectively forcing the swelling ratio $\tilde{J}^{(0)}$ to remain approximately uniform as well. The minor variations in $\tilde{J}^{(0)}$ that occur near the gel-bath interface represent a slight reduction in gel volume due to the loss of anions. The strong Maxwell stresses, which are approximately 100 times greater than the elastic stresses, are responsible for the generation of a large, compressive hoop stress, which leads to the intriguing possibility of localised mechanical instabilities in the double layer.

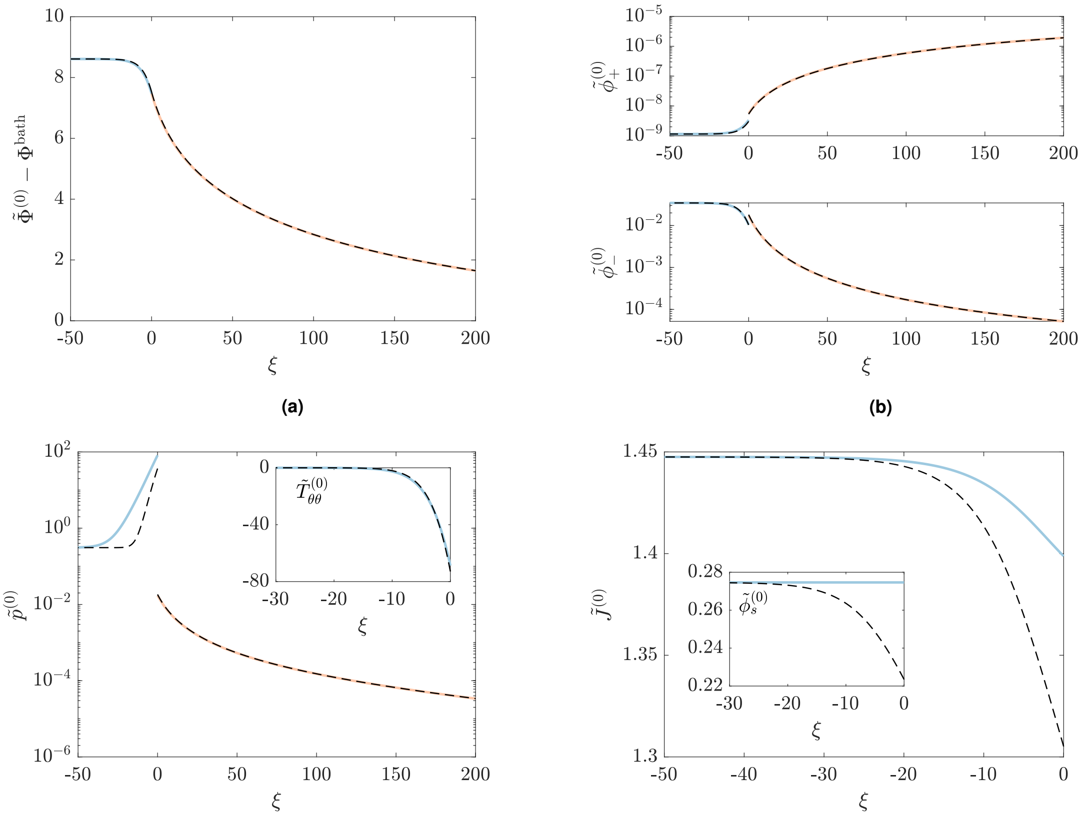

(a) **(b)**

(c) **(d)**

Figure 4: Numerical solution of the inner problem with far-field conditions corresponding to the collapsed state. Solid and dashed lines represent solutions to models with and without interfacial free energy, respectively. Parameters: $\chi = 1.2$, $\mathcal{G} = 0.0005$, $C_f = 0.05$, $\phi_+^{\text{bath}} = 10^{-5}$, $\lambda_z = 1$, $\epsilon_r = 1$, $z_\pm = \pm 1$, and $z_f = 1$.

The dashed lines in Fig. 4 show that neglecting the interfacial free energy does not lead to noticeable changes in the electric potential, ion fractions, and the hoop stress. However, the absence of Korteweg stresses reduces the gel pressure, which is now solely dominated by the Maxwell stresses. There is also a greater decrease in the swelling ratio $\tilde{J}^{(0)}$ now that the solvent fraction can vary across the layer. The decrease in solvent fraction can be rationalised in terms of (98a), which shows that solvent equilibrium in the gel results from a balance between the osmotic pressure $\tilde{\Pi}_s$ and the mechanical pressure $\tilde{p}$. To compensate for the increase in mechanical pressure that arises from the Maxwell stresses, the osmotic pressure must decrease, which drives solvent out of the gel.

In Fig. 5, we show the corresponding numerical solution of the inner problem when the outer solution is in the swollen state. The qualitative features of the solution are similar to those shown in Fig. 4 involving the collapsed state. However, an importance difference is that the double layer in the gel has increased in thickness by a factor of 10 to approximately 100β (or 10 nm). The gradient in the electric potential in the gel is therefore 10 times weaker, resulting in a 100-fold reduction in the Maxwell stresses and, consequently, the total hoop stress. Despite these decreases, the pressure in the gel remains large because of the Korteweg stresses.

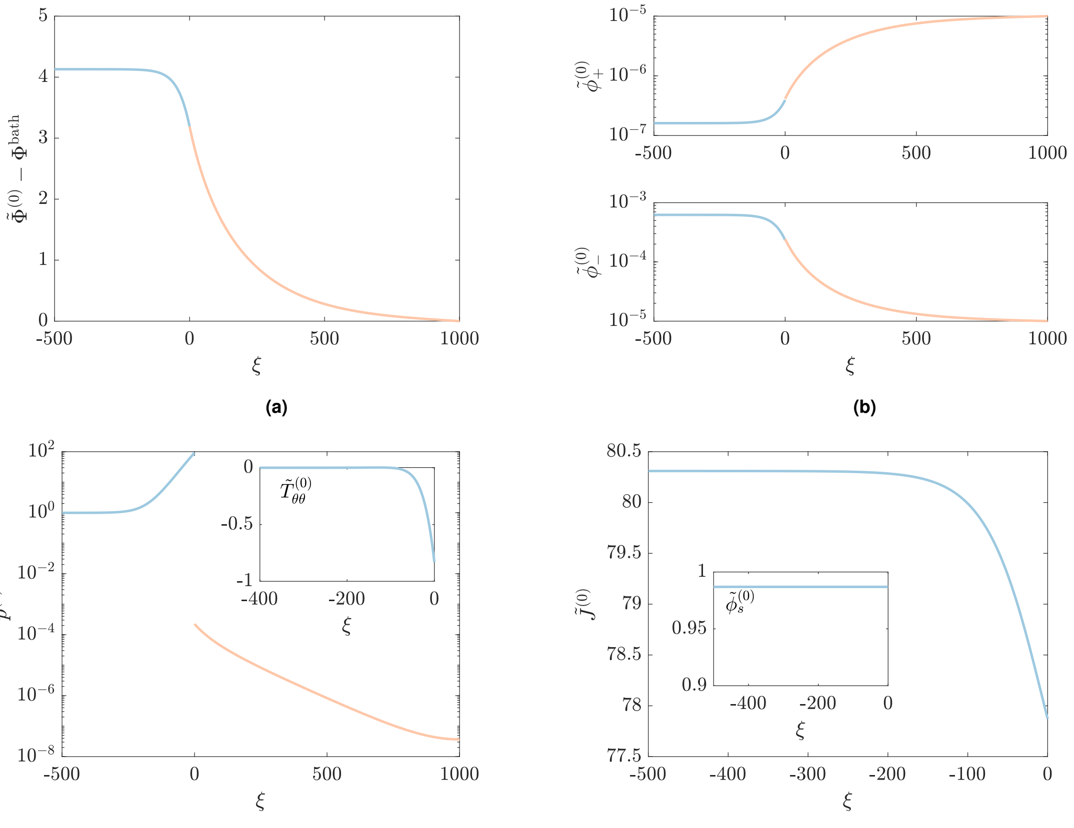

(a) **(b)**

(c) **(d)**

Figure 5: Numerical solution of the inner problem with far-field conditions corresponding to the swollen state. Interfacial free energy is included in the model. Parameter values are the same as in Fig. 4: $\chi = 1.2$, $\mathcal{G} = 0.0005$, $C_f = 0.05$, $\phi_+^{\text{bath}} = 10^{-5}$, $\lambda_z = 1$, $\epsilon_r = 1$, $z_\pm = \pm 1$, and $z_f = 1$.

Using our numerical method, we were unable to solve the inner problem associated with the swollen state when interfacial free energy was neglected. To understand the origin of these numerical difficulties, we considered a second parameter set to reduce the degree of swelling that occurs. This involved increasing the dimensionless shear modulus $\mathcal{G}$, decreasing the Flory interaction parameter χ, and slightly decreasing the nominal concentration of fixed charges C_f. The solution of the outer problem obtained from (104) is shown in Fig. 6 (a) in terms of the equilibrium swelling ratio J^{gel} with $\lambda_z = 1$. For this parameter set there is only a single branch of solutions, corresponding to a gel that monotonically and continuously decreases in volume as the salt fraction in the solution ϕ_+^{bath} increases. We then

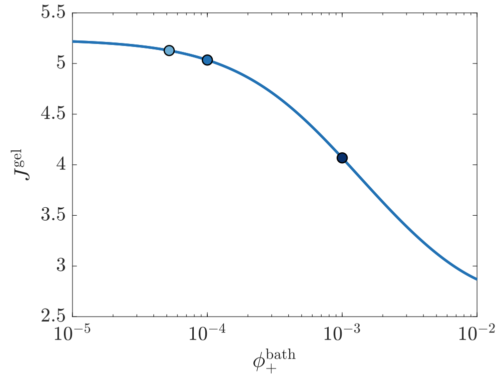

(a)

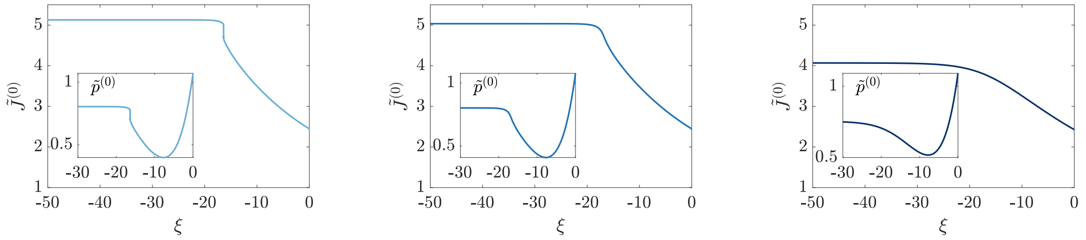

(b) $\phi_+^{\text{bath}} = 5.22 \cdot 10^{-5}$ **(c)** $\phi_+^{\text{bath}} = 10^{-4}$ **(d)** $\phi_+^{\text{bath}} = 10^{-3}$

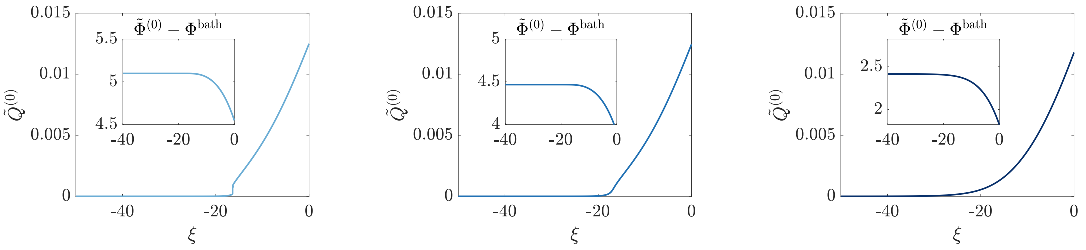

(e) $\phi_+^{\text{bath}} = 5.22 \cdot 10^{-5}$ **(f)** $\phi_+^{\text{bath}} = 10^{-4}$ **(g)** $\phi_+^{\text{bath}} = 10^{-3}$

Figure 6: (a) Equilibrium swelling ratio J^{gel}. (b)–(d) The swelling ratio and pressure across the double layer in the gel at three specific values of ϕ_+^{bath}, marked by circles in panel (a). (e)–(g) The total electric charge (defined in the main text) and electric potential in the gel. Interfacial free energy was not considered when computing the inner solution. Parameter values are: $\chi = 0.7$, $\mathcal{G} = 0.0048$, $C_f = 0.04$, $z_\pm = \pm 1$, $z_f = 1$, $\epsilon_r = 1$, and $\lambda_z = 1$.

solved the inner problem without considering interfacial free energy at three specific values of ϕ^{bath}, marked by filled circles in Fig. 6 (a). The corresponding swelling ratios $\tilde{J}^{(0)}$ are shown in Figs. 6 (b)–(d), with the gel pressure shown in the insets. As the salt fraction in the solution decreases, the far-field swelling ratio increases whereas its value at the gel-bath interface remains pinned at approximately $\tilde{J}^{(0)} \simeq 2.5$. The gradient near the interface therefore steepens with decreasing ϕ_+^{bath} until a sharp front develops when $\phi_+^{\text{bath}} \simeq 5.22 \cdot 10^{-5}$, at which point the swelling ratio appears to become discontinuous. Due to the large change in volume that occurs across the double layer, the radial elastic stresses and the Maxwell stresses are the same order of magnitude, resulting in non-monotonic pressure profiles that also exhibit discontinuous behaviour. The distribution of total charge $\tilde{Q}^{(0)} = \tilde{\phi}_+^{(0)} - \tilde{\phi}_-^{(0)} + z_f \tilde{\phi}_f^{(0)}$ across the double layer of the gel is shown in Figs. 6 (e)–(g), with the electric potential plotted in the inset. For higher salt concentrations, $\phi_+^{\text{bath}} = 10^{-3}$, the total charge smoothly decreases to zero as the distance from the gel-bath interface increases. However, decreasing the salt concentration leads to an abrupt transition between electrically neutral and electrically charged regions. Thus, front formation is associated with a division of the inner problem into two subregions and essentially truncates the double layer, causing it to have finite thickness.

We suspect that the behaviour shown in Fig. 6 is the result of a localised phase transition or mode of phase separation that arises due to the complex interplay between mechanics and electrostatics in the solvent chemical potential (98a). This interplay is absent from the problem when interfacial free energy is included in the model and such that the width of interfacial layers greatly exceeds the width of electric double layers (i.e. in the limit $\omega \gg \beta$). The equilibria that result from phase separation crucially depend on the interfacial energy and neglecting it is a likely explanation for the numerical difficulties encountered when solving the corresponding inner problem.

As a final investigation, we considered an intermediate asymptotic limit, whereby $\omega = \Omega\beta$, with $\Omega = O(1)$ as $\beta \to 0$, that accounts for a small amount of interfacial free energy. Full details of this limit are beyond the scope of this work; however, for the purpose of this discussion it suffices to say that the inner problem in the gel amounts to changing (73) or (98a) to

$$\tilde{\Pi}_s^{(0)} + \mathcal{G}\tilde{p}^{(0)} + \Omega^2 \frac{\partial^2 \tilde{\phi}_s^{(0)}}{\partial \xi^2} = \mu_s^{\text{bath}} \tag{112a}$$

and evaluating the pressure (85) with a Korteweg stress

$$\boldsymbol{n}\cdot\tilde{\mathbf{T}}_K^{(0)}\cdot\boldsymbol{n} = \mathcal{G}^{-1}\Omega^2\left[\tilde{\phi}_s^{(0)}\frac{\partial^2\tilde{\phi}_s^{(0)}}{\partial\xi^2} - \frac{1}{2}\left(\frac{\partial\tilde{\phi}_s^{(0)}}{\partial\xi}\right)^2\right]. \tag{112b}$$

The inner problem is solved for three values of ϕ_+^{bath} and the corresponding swelling ratios $\tilde{J}^{(0)}$ are shown in Fig. 7. The parameter values are identical to those in Fig. 6 aside from $\mathcal{G}$, which has been slightly decreased. In this case, decreasing the salt fraction in the bath triggers the onset of phase separation rather than a single front. Moreover, charge neutrality is violated across the entire inner region, meaning that the inner solution does not match with the homogeneous outer solutions computed from (104). Resolving this issue and further understanding the onset of phase transitions and phase separation near the gel-bath interface will be the focus of an upcoming work.

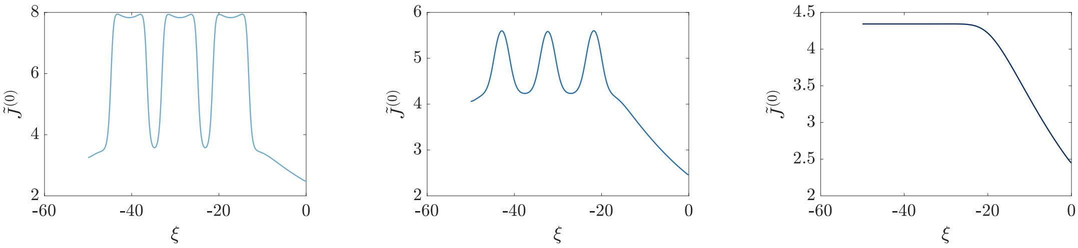

(a) $\phi_+^{\text{bath}} = 10^{-5}$ **(b)** $\phi_+^{\text{bath}} = 6.5 \cdot 10^{-4}$ **(c)** $\phi_+^{\text{bath}} = 10^{-3}$

Figure 7: Phase separation in the inner region. (a)–(c) The swelling ratio at three values of ϕ_+^{bath} computed using an intermediate asymptotic model with a small amount of interfacial free energy. We take $\omega = \Omega\beta$ with $\Omega = 10^{-1}$. The remaining parameters are: $\chi = 0.7$, $\mathcal{G} = 0.004$, $C_f = 0.04$, $z_\pm = \pm 1$, $z_f = 1$, $\epsilon_r = 1$, and $\lambda_z = 1$.

7 Conclusions

In this paper we use a combination of asymptotic and numerical methods to study the electrical double layers that form at the interface between an ionic solvent bath and a polyelectrolyte gel. The inclusion of interfacial energy in the model yields a new small parameter, ω, that measures the thickness of the internal interfaces, as part of our matched asymptotic analysis. In the current analysis, we considered the thickness of the Debye layer β to be the smallest parameter in the problem, i.e. $\omega \gg \beta$. As a limiting and comparative case, we also carried out the asymptotic analysis when the interfacial energy is neglected, i.e. when $\omega = 0$ (in Sec. 4). For the setting of a swelling gel in cylindrical geometry, we have investigated contributions to the solutions of the new electroneutral models and identified several novel features such as formation of internal layers within the Debye layer. Here we also briefly touch upon the case when $\omega = O(\beta)$ (in Sec. 6).

Our analysis of the double layer between a polyelectrolyte gels and an ionic bath reveals a much more complex structure as has been thought before. In the future, further asymptotic limits, identified in this study and only briefly touched upon, will be investigated in detail in our upcoming work. This will be fundamental for understanding the subtle nature of the limiting processes that yield consistent jump conditions for electroneutral models that hold across interfaces with potentially complex and dynamic double layers. Recalling the large body of applied literature where electroneutral models have been used, our studies will open doors to discovery and quantitative understanding of pattern formation in polyelectrolyte gels.

The interesting novel behaviour of phase separation within the Debye layer will be studied further, adding new insights on internal gel-gel phase separation that has been observed in our own studies [4] as well as to earlier work by [16], or [28], based on a different theoretical approach, where transitions from phase segregation of lamellar nanostructures to the phase separation of a collapsed gel is investigated.

A Summary of the governing equations in dimensional form

A.1 Bulk equations for the gel

Conservation of solvent and ions is given by

$$\frac{\partial c_m}{\partial t} + \nabla \cdot (c_m \boldsymbol{v}_m) = 0 \tag{113}$$

for $m \in \mathbb{M}$, where c_m is the (current) concentration (number of molecules per unit current volume). The velocity $\boldsymbol{v}_m$ is related to the network velocity $\boldsymbol{v}_n$ and the diffusive flux $\boldsymbol{j}_m$ according to

$$c_m(\boldsymbol{v}_m - \boldsymbol{v}_n) = \boldsymbol{j}_m. \tag{114}$$

Due to incompressibility, the determinant of the deformation tensor is

$$J = 1 + \sum_{m\in\mathbb{M}} \nu C_m = \left(1 - \sum_{m\in\mathbb{M}} \nu c_m\right)^{-1}, \tag{115}$$

where $C_m = Jc_m$ is the nominal concentration of each mobile species and ν is the molecular volume, i.e. the volume of an individual molecule. For simplicity, we assume that all of the molecules are roughly the same size. The diffusive fluxes of the solvent and ions are given by

$$\boldsymbol{j}_s = -\frac{D_s(J)}{k_B T} \sum_{m\in\mathbb{M}} c_m \nabla \mu_m, \tag{116a}$$

$$\boldsymbol{j}_\pm = -\frac{D_\pm c_\pm}{k_B T} \nabla \mu_\pm + \frac{c_\pm}{c_s} \boldsymbol{j}_s, \tag{116b}$$

where T is temperature, k_B is Boltzmann's constant, D_s is the diffusivity of solvent in a polymer network, and $D_\pm$ are the diffusivity of ions in a pure solvent bath. The chemical potential of solvent can be written as

$$\mu_s = \mu_s^0 + \nu(p + \Pi_s) - \gamma\nabla^2 c \tag{117}$$

where p is the mechanical pressure, Π_s is the osmotic pressure of the solvent,

$$\Pi_s = \frac{k_B T}{\nu}\left[\log(\nu c_s) + \frac{\chi(1-\nu c_s)}{J} + \frac{1}{J}\right], \tag{118}$$

and χ is the Flory interaction parameter. The chemical potential of ions is given by

$$\mu_\pm = \mu_\pm^0 + \nu(\Pi_\pm + p) \pm e\Phi, \tag{119}$$

where Φ is the electric potential, e is the elementary charge, and $\Pi_\pm$ is the osmotic pressure

$$\Pi_\pm = \frac{k_B T}{\nu}\left[\log(\nu c_\pm) + \frac{1}{J}(1-\chi\nu c_s)\right]. \tag{120}$$

The quantities μ_m^0 are reference values of the chemical potential. The electric potential satisfies

$$-\epsilon^{\text{gel}}\nabla^2\Phi = e(c_+ - c_- + z_f c_f) \tag{121}$$

where ϵ^{gel} is the electrical permittivity of the gel and c_f is the current concentration of fixed charges. Mechanical equilibrium leads to

$$\nabla\cdot\mathbf{T} = 0, \tag{122}$$

where the Cauchy stress tensor $\mathbf{T}$ can be decomposed into four contributions

$$\mathbf{T} = \mathbf{T}_e + \mathbf{T}_K + \mathbf{T}_M - p\mathbf{I}, \tag{123}$$

associated with the elastic stress $\mathbf{T}_e$, the Korteweg stress $\mathbf{T}_K$, the Maxwell stress $\mathbf{T}_M$, and the isotropic fluid pressure. These three stress tensors are given by

$$\mathbf{T}_e = GJ^{-1}(\mathbf{B} - \mathbf{I}), \tag{124a}$$

$$\mathbf{T}_K = \gamma\left[\left(\frac{1}{2}|\nabla c_s|^2 + c_s\nabla^2 c_s\right)\mathbf{I} - \nabla c_s\otimes\nabla c_s\right], \tag{124b}$$

$$\mathbf{T}_M = \epsilon^{\text{gel}}\left(\nabla\Phi\otimes\nabla\Phi - \frac{1}{2}|\nabla\Phi|^2\mathbf{I}\right), \tag{124c}$$

where G and γ play the role of a shear modulus and surface energy, respectively. The left Cauchy–Green tensor is defined as $\mathbf{B} = \mathbf{F}\mathbf{F}^T$. In Eulerian coordinates, the deformation gradient tensor is related to the displacement $\boldsymbol{a}$ via the relation

$$\mathbf{F}^{-1} = \mathbf{I} - \nabla\boldsymbol{a}. \tag{125}$$

The velocity of the network can be determined from

$$\boldsymbol{v}_n = \mathbf{F}\,\frac{\partial\boldsymbol{a}}{\partial t}. \tag{126}$$

A.2 Governing equations for the bath

Conservation of solvent and ions is given by

$$\frac{\partial c_m}{\partial t} + \nabla \cdot (c_m \boldsymbol{v}_m) = 0, \tag{127}$$

for $m \in \mathbb{M}$. The mixture velocity is defined as

$$\boldsymbol{v} = \sum_m \nu c_m \boldsymbol{v}_m. \tag{128}$$

Note that we also have

$$\sum_m \nu c_m = 1, \quad \nabla \cdot \boldsymbol{v} = 0. \tag{129}$$

The velocity of each species can be linked to the diffusive flux via

$$c_m(\boldsymbol{v}_m - \boldsymbol{v}) = \boldsymbol{q}_m, \tag{130}$$

which implies that

$$\sum_{m \in \mathbb{M}} \boldsymbol{q}_m = 0. \tag{131}$$

The diffusive fluxes are defined by

$$\boldsymbol{j}_\pm = -\frac{D_\pm c_\pm}{k_B T}\left(\nabla \mu_\pm - \nu \sum_{m \in \mathbb{M}} c_m \nabla \mu_m\right) + \frac{c_\pm}{c_s}\boldsymbol{j}_s, \tag{132a}$$

$$\boldsymbol{j}_s = -\boldsymbol{j}_+ - \boldsymbol{j}_-. \tag{132b}$$

The chemical potentials are given by

$$\mu_s = \mu_s^0 + \nu(\Pi_s + p), \tag{133a}$$

$$\mu_\pm = \mu_\pm^0 + \nu(\Pi_\pm + p) \pm e\Phi, \tag{133b}$$

where

$$\Pi_m = \frac{k_B T}{\nu} \log(\nu c_m). \tag{134}$$

The electric potential satisfies

$$-\epsilon^{\text{bath}} \nabla^2 \Phi = e(c_+ - c_-). \tag{135}$$

The stress balance in the bath is given by

$$\nabla \cdot \mathbf{T} = 0, \tag{136}$$

where $\mathbf{T} = \mathbf{T}_v + \mathbf{T}_M - p\mathbf{I}$ where

$$\mathbf{T}_v = \eta(\nabla \boldsymbol{v} + \nabla \boldsymbol{v}^T), \tag{137a}$$

$$\mathbf{T}_M = \epsilon^{\text{bath}}\left(\nabla\Phi \otimes \nabla\Phi - \frac{1}{2}|\nabla\Phi|^2 \mathbf{I}\right). \tag{137b}$$

A.3 Boundary conditions at the gel-bath interface

The boundary conditions are discussed in detail in the text. Conservation of solvent and ions across the gel-bath interface are given by

$$[c_m(\boldsymbol{v}_m \cdot \boldsymbol{n} - V_n)]_{\boldsymbol{x}=\boldsymbol{r}^-}^{\boldsymbol{x}=\boldsymbol{r}^+} = 0, \tag{138}$$

where V_n is the normal velocity of the interface. The kinematic boundary condition for the velocity of the polymer network is

$$[\boldsymbol{v}_n \cdot \boldsymbol{n} - V_n]_{\boldsymbol{x}=\boldsymbol{r}^-} = 0. \tag{139}$$

Continuity of chemical potential implies that

$$[\mu_m]_{\boldsymbol{x}=\boldsymbol{r}^-}^{\boldsymbol{x}=\boldsymbol{r}^+} = 0. \tag{140}$$

The variational condition for the solvent concentration is

$$[\nabla c_s \cdot \boldsymbol{n}]_{\boldsymbol{x}=\boldsymbol{r}^-} = 0. \tag{141}$$

Conservation of normal and tangential momentum gives

$$[\mathsf{T} \cdot \boldsymbol{n}]_{\boldsymbol{x}=\boldsymbol{r}^+}^{\boldsymbol{x}=\boldsymbol{r}^+} = 0. \tag{142}$$

The slip condition reads as

$$[\boldsymbol{v} \cdot \boldsymbol{t}_i]_{\boldsymbol{x}=\boldsymbol{r}^-}^{\boldsymbol{x}=\boldsymbol{r}^+} = 0. \tag{143}$$

We impose continuity of electrical potential and electric displacement

$$[\Phi]_{\boldsymbol{x}=\boldsymbol{r}^-}^{\boldsymbol{x}=\boldsymbol{r}^+} = 0, \tag{144a}$$

$$[-\epsilon\nabla\Phi \cdot \boldsymbol{n}]_{\boldsymbol{x}=\boldsymbol{r}^-}^{\boldsymbol{x}=\boldsymbol{r}^+} = 0. \tag{144b}$$

and therefore do not account for surface charges on the gel.

B Conventions and identities

A vector $\boldsymbol{v}$ is written in component form as $\boldsymbol{v} = v_i\boldsymbol{e}_i$. Similarly, a tensor T is written in component form as $\mathsf{T} = \mathsf{T}_{ij}\boldsymbol{e}_i \otimes \boldsymbol{e}_j$. The gradient of the vector $\boldsymbol{v}$ is defined as

$$\nabla\boldsymbol{v} = \frac{\partial}{\partial\xi_j}(v_i\boldsymbol{e}_i) \otimes \boldsymbol{e}_j. \tag{145}$$

The tensor divergence is defined as

$$\nabla \cdot \mathsf{T} = \frac{\partial}{\partial\xi_i}(\mathsf{T}_{jk}\boldsymbol{e}_j \otimes \boldsymbol{e}_k)\,\boldsymbol{e}_i, \tag{146}$$

which can be evaluated using the property of the dyadic product $(\boldsymbol{a} \otimes \boldsymbol{b})\boldsymbol{c} = (\boldsymbol{b} \cdot \boldsymbol{c})\boldsymbol{a}$. Given two vectors $\boldsymbol{a}$ and $\boldsymbol{b}$ and a tensor T, we write

$$\boldsymbol{a} \cdot \mathsf{T} \cdot \boldsymbol{b} = a_i\mathsf{T}_{ij}b_j. \tag{147}$$

C Transformation of the derivatives in the inner region

In the inner problem we write

$$\boldsymbol{x} = \boldsymbol{r}(s_1, s_2, t) + \beta\xi\boldsymbol{n}(s_1, s_2, t), \tag{148a}$$

$$t = t', \tag{148b}$$

where $\boldsymbol{r}$ denotes the location of the gel-bath interface and $\boldsymbol{n}$ is the unit normal vector pointing from the gel into the bath. The tangent and normal vectors are defined as

$$\boldsymbol{t}_i = \frac{\partial \boldsymbol{r}}{\partial s_i}, \quad \boldsymbol{n} = \frac{\boldsymbol{t}_1 \times \boldsymbol{t}_2}{\|\boldsymbol{t}_1 \times \boldsymbol{t}_2\|}. \tag{149}$$

The normal velocity of the interface is defined as $V_n = \boldsymbol{n} \cdot \partial_t \boldsymbol{r}$.

Before proceeding with the transformation, it is helpful to summarise some key definitions and results from differential geometry. The components of the metric tensor are defined as $g_{ij} = \boldsymbol{t}_i \cdot \boldsymbol{t}_j$. We let g^{ab} denote the components of the inverse of the metric tensor. The curvature tensor has components

$$K_{ij} = -\boldsymbol{n} \cdot \frac{\partial \boldsymbol{t}_i}{\partial s_j} = \frac{\partial \boldsymbol{n}}{\partial s_j} \cdot \boldsymbol{t}_i. \tag{150}$$

The metric tensor, its inverse, and the curvature tensor are all symmetric. The shape operator is defined as $S^a_j = g^{ai} K_{ij}$. The eigenvalues of the shape operator, κ_1 and κ_2, define the principal curvatures of the surface. Similarly, the trace of the shape operator is related to the mean curvature of the surface, $\kappa = (\kappa_1 + \kappa_2)/2$, through the relation $S^a_a = 2\kappa$. By ensuring that the normal vector $\boldsymbol{n}$ computed from (149) points into the bath, the principal curvatures of a spherical gel will be positive.

A straightforward application of the chain rule shows that

$$\frac{\partial}{\partial s_i} = \left(\boldsymbol{t}_i + \beta\xi \frac{\partial \boldsymbol{n}}{\partial s_i}\right) \cdot \nabla, \tag{151}$$

$$\frac{\partial}{\partial \xi} = \beta \boldsymbol{n} \cdot \nabla, \tag{152}$$

$$\frac{\partial}{\partial t'} = \frac{\partial}{\partial t} + \left(\frac{\partial \boldsymbol{r}}{\partial t} + \beta\xi \frac{\partial \boldsymbol{n}}{\partial t}\right) \cdot \nabla. \tag{153}$$

We now exploit the fact that $\beta \ll 1$ and write the differential operators ∇ and ∂_t as asymptotic series of the form $\nabla = \beta^{-1}\nabla^{(-1)} + \nabla^{(0)} + \beta\nabla^{(1)} + O(\beta^2)$ and $\partial_t = \beta^{-1}\partial_t^{(-1)} + O(1)$. We do not calculate the higher-order contributions to the time derivative because they are not necessary for the asymptotic analysis.

The $O(\beta^{-1})$ problem for the del operator is

$$0 = \boldsymbol{t}_i \cdot \nabla^{(-1)}, \tag{154a}$$

$$\frac{\partial}{\partial \xi} = \boldsymbol{n} \cdot \nabla^{(-1)}, \tag{154b}$$

which has the solution

$$\nabla^{(-1)} = \boldsymbol{n} \frac{\partial}{\partial \xi}. \tag{155}$$

The corresponding problem for the time derivative is trivial to solve and has solution

$$\partial_t^{(-1)} = -V_n \frac{\partial}{\partial \xi}. \tag{156}$$

The $O(1)$ problem for the del operator is given by

$$\frac{\partial}{\partial s_i} = \boldsymbol{t}_i \cdot \boldsymbol{\nabla}^{(0)} + \xi \boldsymbol{n} \cdot \frac{\partial \boldsymbol{n}}{\partial s_i}\frac{\partial}{\partial \xi}, \tag{157a}$$

$$0 = \boldsymbol{n} \cdot \nabla^{(0)}. \tag{157b}$$

Since $\boldsymbol{n}$ is a unit vector, we have that $\boldsymbol{n} \cdot \partial_{s_i}\boldsymbol{n} = (1/2)\partial_{s_i}(\boldsymbol{n}\cdot\boldsymbol{n}) = 0$, implying the final term in (157a) vanishes. Equation (157b) implies that $\nabla^{(0)}$ lies in the tangent plane and thus has the form $\nabla^{(0)} = a_i \boldsymbol{t}_i$. Inserting this solution in (157a) and solving gives

$$\nabla^{(0)} = g^{ij}\boldsymbol{t}_i \frac{\partial}{\partial s_j} \equiv \nabla_s, \tag{158}$$

where ∇_s is the surface gradient.

The $O(\beta)$ problem for the del operator, after minor simplification, is given by

$$\boldsymbol{t}_i \cdot \nabla^{(1)} = -\xi \frac{\partial \boldsymbol{n}}{\partial s_i} \cdot \nabla^{(0)}, \tag{159a}$$

$$\boldsymbol{n} \cdot \nabla^{(1)} = 0. \tag{159b}$$

By following the same strategy as the $O(1)$ problem, substituting the solution in (158), and using (150) and the definition of the shape operator, we find that

$$\nabla^{(1)} = -\xi S^i_p g^{pj} \boldsymbol{t}_i \frac{\partial}{\partial s_j}. \tag{160}$$

Using these asymptotic expansions, we can construct the Laplacian $\nabla^2 = \nabla \cdot \nabla$. In doing so, we will use the fact that the tangent and normal vectors $\boldsymbol{t}_i$ and $\boldsymbol{n}$ are independent of the coordinate ξ. As a result, $\nabla^{(-1)} \cdot \nabla^{(-1)} = \partial_{\xi\xi}$, $\nabla^{(-1)} \cdot \nabla^{(0)} = 0$, and $\nabla^{(-1)} \cdot \nabla^{(1)} = 0$. Moreover,

$$\nabla^{(0)} \cdot \nabla^{(-1)} = g^{ij}\boldsymbol{t}_i \cdot \frac{\partial \boldsymbol{n}}{\partial s_j}\frac{\partial}{\partial \xi} = S^i_i \frac{\partial}{\partial \xi} = 2\kappa \frac{\partial}{\partial \xi}, \tag{161a}$$

$$\nabla^{(0)} \cdot \nabla^{(0)} = g^{ij}\boldsymbol{t}_i \cdot \frac{\partial}{\partial s_j}\left(g^{pq}\boldsymbol{t}_p \frac{\partial}{\partial s_q}\right) = g^{ij}g^{pq}\, \boldsymbol{t}_i \cdot \frac{\partial \boldsymbol{t}_p}{\partial s_j}\frac{\partial}{\partial s_q} + \frac{\partial}{\partial s_p}\left(g^{pq}\frac{\partial}{\partial s_q}\right). \tag{161b}$$

In order to simplify (161b), we express the derivatives of the tangent vectors as

$$\frac{\partial \boldsymbol{t}_p}{\partial s_j} = \Gamma^a_{pj}\boldsymbol{t}_a - K_{pj}\boldsymbol{n}, \tag{162}$$

where Γ^a_{pj} is the Christoffel symbol. In addition, we invoke the identity

$$\Gamma^j_{pj} = \frac{1}{\sqrt{g}}\frac{\partial}{\partial s_p}\left(\sqrt{g}\right), \tag{163}$$

where $g = g_{11}g_{22} - g_{12}^2$ is the determinant of the metric tensor. Thus, we find that $\nabla^{(0)} \cdot \nabla^{(0)} = \nabla_s^2$, where

$$\nabla_s^2 = \frac{1}{\sqrt{g}} \frac{\partial}{\partial s_p} \left(\sqrt{g} g^{pq} \frac{\partial}{\partial s_q} \right) \tag{164}$$

is the surface Laplacian (or Laplace–Beltrami operator). Finally, we have that

$$\nabla^{(1)} \cdot \nabla^{(-1)} = -\xi S_p^i g^{pj} \, \boldsymbol{t}_i \cdot \frac{\partial \boldsymbol{n}}{\partial s_j} \frac{\partial}{\partial \xi} = -\xi S_p^i g^{pj} K_{ij} \frac{\partial}{\partial \xi} = -\xi S_p^i S_i^p \frac{\partial}{\partial \xi} = -\xi(\kappa_i \kappa_i) \frac{\partial}{\partial \xi}. \tag{165}$$

The last equality is obtained by noticing that $S_p^i S_i^p$ is the trace of the square of the shape operator and thus $S_p^i S_i^p = \kappa_i \kappa_i$.

References

[1] T. Bertrand, J. Peixinho, S. Mukhopadhyay, and C. W. MacMinn. Dynamics of swelling and drying in a spherical gel. *Physical Review Applied*, 6(6):064010, 2016.

[2] D. Caccavo, S. Cascone, G. Lamberti, and A. A. Barba. Hydrogels: experimental characterization and mathematical modelling of their mechanical and diffusive behaviour. *Chem. Soc. Rev.*, 47:2357–2373, 2018.

[3] G. L. Celora, M. G. Hennessy, A. Münch, B. Wagner, and S. Waters. A kinetic model of a polyelectrolyte gel undergoing phase separation. *Submitted*, 2020.

[4] G. L. Celora, M. G. Hennessy, A. Münch, S. L. Waters, and B. Wagner. Spinodal decomposition and collapse of a polyelectrolyte gel. *Submitted*, 2020.

[5] C. J. Chan, W. Li, G. Cojoc, and J. Guck. Volume transitions of isolated cell nuclei induced by rapid temperature increase. *Biophysical Journal*, 112(6):1063 – 1076, 2017.

[6] J. P. de Souza and M. Z. Bazant. Continuum theory of electrostatic correlations at charged surfaces. *The Journal of Physical Chemistry C*, 124(21):11414–11421, 2020.

[7] M. S. Dimitriyev, Y.-W. Chang, P. M. Goldbart, and A. Fernández-Nieves. Swelling thermodynamics and phase transitions of polymer gels. *Nano Futures*, 3(4):042001, oct 2019.

[8] M. Doi and M. Makino. Electrokinetic boundary condition compatible with the onsager reciprocal relation in the thin double layer approximation. *The Journal of Chemical Physics*, 128(4):044715, 2008.

[9] F. G. Donnan. The Theory of Membrane Equilibria. *Chemical Reviews*, 1(1):73–90, 1924.

[10] A. D. Drozdov, A. A. Papadimitriou, J. H. Liely, and C. G. Sanporean. Constitutive equations for the kinetics of swelling of hydrogels. *Mechanics of Materials*, 2016.

[11] A. R. Farooqi, J. Zimmermann, R. Bader, and U. van Rienen. Numerical simulation of electroactive hydrogels for cartilageâĂŞtissue engineering. *Materials*, 12(18), 2019.

[12] M. G. Hennessy, A. Münch, and B. Wagner. Phase separation in swelling and deswelling hydrogels with a free boundary. *Phys. Rev. E*, 101:032501, Mar 2020.

[13] W. Hong, X. Zhao, and Z. Suo. Large deformation and electrochemistry of polyelectrolyte gels. *Journal of the Mechanics and Physics of Solids*, 58(4):558–577, apr 2010.

[14] F. Horkay, I. Tasaki, and P. J. Basser. Effect of monovalent-divalent cation exchange on the swelling of polyacrylate hydrogels in physiological salt solutions. *Biomacromolecules*, 2(1):195–199, 2001.

[15] D. Komoto, T. Furuike, and H. Tamura. Preparation of polyelectrolyte complex gel of sodium alginate with chitosan using basic solution of chitosan. *International Journal of Biological Macromolecules*, 126:54 – 59, 2019.

[16] E. Y. Kramarenko and A. R. Khokhlov. Intranetwork phase separation in polyelectrolyte gels. *Polymer Gels and Networks*, 6(1):45 – 56, 1998.

[17] H. J. Kwon, Y. Osada, and J. P. Gong. Polyelectrolyte gels-fundamentals and applications. *Polymer Journal*, 38(12):1211–1219, nov 2006.

[18] D. W. Lee, D. J. Im, and I. S. Kang. Electric double layer at the interface of ionic liquidâĂŞdielectric liquid under electric field. *Langmuir*, 29(6):1875–1884, 2013.

[19] J. Li and D. Mooney. Designing hydrogels for controlled drug delivery. *Nature Reviews Materials*, 1:16071, 2016.

[20] Y. Mori, H. Chen, C. Micek, and M.-C. Calderer. A dynamic model of polyelectrolyte gels. *SIAM Journal on Applied Mathematics*, 73(1):104–133, 2013.

[21] T. Nakajima, T. Chida, K. Mito, T. Kurokawa, and J. P. Gong. Double-network gels as polyelectrolyte gels with salt-insensitive swelling properties. *Soft Matter*, 16:5487–5496, 2020.

[22] K. K. Nakashima, M. A. Vibhute, and E. Spruijt. Biomolecular chemistry in liquid phase separated compartments. *Frontiers in Molecular Biosciences*, 6:21, 2019.

[23] I. Ohmine and T. Tanaka. Salt effects on the phase transition of ionic gels. *The Journal of Chemical Physics*, 77(11):5725–5729, 1982.

[24] G. Richardson and J. R. King. Time-dependent modelling and asymptotic analysis of electrochemical cells. *Journal of Engineering Mathematics*, 59:239 – 275, 2007.

[25] T. K. Sherwood, R. L. Pigford, and C. R. Wilke. *Mass transfer*. McGraw-Hill Book Co, New York, 1975.

[26] T. M. Squires and M. Z. Bazant. Induced-charge electro-osmosis. *Journal of Fluid Mechanics*, 509:217âĂŞ252, 2004.

[27] X. Wang, W. Hong, et al. Surface interactions between two like-charged polyelectrolyte gels. *Physical Review E*, 81(4):041803, 2010.

[28] K.-A. Wu, P. K. Jha, and M. O. de la Cruz. Control of nanophases in polyelectrolyte gels by salt addition. *Macromolecules*, 43(21):9160–9167, 2010.

[29] T. Yamamoto and M. Doi. Electrochemical mechanism of ion current rectification of polyelectrolyte gel diodes. *Nat. Commun.*, 5:4162, 2014.

[30] E. Yariv. An asymptotic derivation of the thin-Debye-layer limit for electrokinetic phenomena. *Chemical Engineering Communications*, 197(1):3–17, 2009.

[31] E. Yariv, O. Schnitzer, and I. Frankel. Streaming-potential phenomena in the thin-debye-layer limit. part 1. general theory. *Journal of Fluid Mechanics*, 685:306–334, 2011.

[32] Y. Yu, C. M. Landis, and R. Huang. Salt-induced swelling and volume phase transition of polyelectrolyte gels. *Journal of Applied Mechanics*, 84(5):051005, 2017.